



Fibonacci wavelet collocation method for the numerical approximation of fractional order Brusselator chemical model

G. Manohara¹ · S. Kumbinarasaiah¹

Received: 24 April 2023 / Accepted: 13 September 2023
© The Author(s), under exclusive licence to Springer Nature Switzerland AG 2023

Abstract

This research study's primary goal is to create an efficient wavelet collocation technique to resolve a kind of nonlinear fractional order systems of ordinary differential equations that arise in the modeling of autocatalytic chemical reaction problems. Here, we created the functional matrix of integration for the Fibonacci wavelets. The Fibonacci wavelet collocation method is employed to find the numerical solution of the system of nonlinear coupled ordinary differential equations of both integer and fractional order. The nonlinear Brusselator system is transformed into an algebraic equation system using the operational matrices of fractional derivative and collocation technique. These algebraic equations are treated by the Newton–Raphson method, and obtained unknown coefficient values are substituted in the approximation. We demonstrate our method's computational effectiveness and accuracy using different model constraints in the numerical examples. The effectiveness and consistency of the developed strategy's performance are shown in graphs and tables. Comparisons with existing methods available in the literature demonstrate the high accuracy and robustness of the developed Fibonacci wavelet collocation method. Mathematical software Mathematica has been used to perform all calculations.

Keywords Brusselator chemical model · Collocation technique · Fibonacci wavelet · Riemann–Liouville fractional derivative · System of fractional differential equations (SFDEs)

Mathematics Subject Classification 34B16 · 34A12 · 6L05 · 65L10

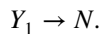
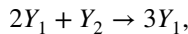
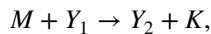
✉ S. Kumbinarasaiah
kumbinarasaiah@gmail.com

G. Manohara
manoharavdc15@gmail.com

¹ Department of Mathematics, Bangalore University, Bengaluru 560 056, India

1 Introduction

In 1968, Prigogine and Lefever [1] introduced the Brusselator model. It is also known as the Belousov–Zhabotinsky model. A theoretical representation of an autocatalytic process is the Brusselator. This model represents a typical nonlinear reaction in which a reactant species interacts with other species to boost its production rate. The chemical reaction's constituents are denoted by $Y_1, Y_2, K, L, M,$ and N . The reaction procedure can generally be broken down into the subsequent four stages.



Our current presumption is that species L and M are readily accessible and can be modeled at a constant concentration. Furthermore, observe that the reaction's end products, N and K , are eliminated after creation. Under scaling the rate constant to unity, the rate equations become as follows.

$$\left. \begin{aligned} \frac{d(Y_1)}{d\zeta} &= \{L\} + \{Y_1^2\}\{Y_2\} - \{M\}\{Y_1\} - \{Y_1\} \\ \frac{d(Y_2)}{d\zeta} &= \{M\}\{Y_1\} - \{Y_1^2\}\{Y_2\} \end{aligned} \right\} \quad (1)$$

Fractional differential equations (FDEs) are equations with arbitrary (fractional) order variables. Differential equations of fractional order are naturally generated by mathematical modeling based on improved rheological models. This idea generalizes the classical differential equations. Many works have been published where fractional derivatives describe better material properties, particularly in the theory of viscoelasticity and hereditary solid mechanics. Fractional derivatives offer a fantastic tool for describing diverse materials and processes' memory and inherited characteristics. It has been discovered that non-integer derivatives and integrals are better suited to describe the characteristics of several actual processes and materials. A more comprehensive range of behaviors can be modeled by switching from integer-order to fractional derivatives. It has been discovered that the fractional order system theory may accurately describe the behavior of many physical systems. Fractional order differential equations have drawn much attention from researchers due to their frequent appearance in numerous uses in biology, acoustics, robotics, signal processing, fluid mechanics, physics, engineering, and viscoelasticity. As a result, solving fractional integral equations, fractional partial differential equations, and fractional ordinary differential equations of physical interest has received a lot of attention. Fractional Differential Equations (FDEs) have also been used to model numerous physical and engineering problems. Determining the exact solutions to

physical phenomena is crucial to better understanding and applying them in scientific research.

A few semi-analytical techniques, including the Adomian decomposition approach [2], the Homotopy analysis method [3], the Homotopy asymptotic method [4], the multistep fractional differential transform method [5], and the Homotopy perturbation method [6] have been suggested to analytically approximate nonlinear fractional differential equations. Sadly, these approaches have limitations and cannot ensure the high-precision solution of complicated fractional differential equations across the broad, especially in the unbounded domain. Hence, numerical methods have a definite advantage over analytical methods. Analytical methods, however, still hold particular importance if they can produce reliable results. Approximation and numerical approaches are widely utilized because most fractional differential equations lack exact analytic solutions. Developing precise and effective procedures for solving FDEs has been a focus of active study. For a long time, a core concept in numerical and computational mathematics has been the numerical solution of differential equations of integer order.

Our primary objective is to investigate the fractional part of the Brusselator model. Based on the (fractional) version of wavelet functions used in matrix formulation, an approximation of the solution to the following nonlinear fractional-order Brusselator system of two equations is given in this research.

$$\left. \begin{aligned} D^\alpha Y_1(\zeta) &= \lambda - (\delta + 1)Y_1(\zeta) + Y_2^2(\zeta)Y_1(\zeta) \\ D^\beta Y_2(\zeta) &= \delta Y_1(\zeta) - Y_2^2(\zeta)Y_1(\zeta) \end{aligned} \right\} \quad \zeta \in [0, 1] \quad (2)$$

With the initial conditions of the above system, given by $Y_1(0) = u_0$, $Y_2(0) = v_0$.

Where λ and δ are two positive real numbers. D^α , D^β represents the Riemann–Liouville fractional derivatives of order $\alpha \in (0, 1]$. The classical Brusselator system (1) will be obtained if we fix $\alpha = \beta = 1$. Numerous researchers from various perspectives on dynamic systems and numerical behaviors have examined the fractional-order system (2) in the literature. To numerically solve (2), the authors of [7, 8] created some nonstandard finite difference (NSFD) techniques. The variational iteration technique is developed as a semi-analytical approach in [9]. In [10], the polynomial least squares method (PLSM) was examined. Bernstein and Legendre wavelet-based operational matrix techniques were investigated in [11, 12]. The fractional clique collocation technique is applied in [13]. In [14, 15], the stability of the fractional Brusselator system was discussed. The Brusselator model with fractional derivatives in the senses of Caputo-Fabrizio, Liouville-Caputo, and Atangana-Baleanu was recently considered [16]. Fractional series solution construction for the nonlinear fractional Brusselator model was carried out in [17], W Beghami et al. applied the Laplace-optimized decomposition approach in [18], and Anber et al. proposed the Adomian decomposition method in [19].

Wavelets are a mathematical tool for information extraction from a wide range of data types. To thoroughly analyze data, sets of wavelets are required. Wavelets mathematically deconstruct a signal without gaps or overlaps, reversing the decomposition process. Since retrieving the original information with as little loss as possible is preferred, sets of wavelets are helpful in wavelet-based compression/

decompression techniques. Wavelet holds the multi-resolution analysis that divide a signal into many frequency bands. A multiresolution analysis (MRA) is the design method of most of the practically relevant discrete wavelet transforms (DWT) and the justification for the algorithm of the fast wavelet transform (FWT). It was introduced in this context in 1988 by Stephane Mallat, Yves Meyer, and his predecessors in the microlocal analysis in the theory of differential equations. Wavelets have several characteristics that support their application in numerically solving differential equations. The orthogonal, compactly supported wavelet basis precisely approximates an increasingly higher-order polynomial. This wavelet-based representation of differential operations can be precise and stable even in areas with significant gradients or oscillations. Orthogonal wavelet basis also has the advantage of multi-resolution analysis over conventional techniques. For some of the common mathematical problems, various wavelet collocation techniques have been used, such as the Chebyshev wavelet collocation method [20], collocation method based on Bernoulli and Gegenbauer wavelets [21], Hermite wavelet collocation method [22], Laguerre wavelet collocation method [23]. Several wavelet collocation techniques are typically employed to solve fractional differential equations, which include Chelyshkov wavelets [24], Cubic B Spline [25], Genocchi wavelets [26], Taylor wavelets [27], Haar wavelets [28, 29], Bernoulli wavelets [30–32], Hermite wavelets [33], Legendre wavelets and Legendre wavelet tau method [34–36], Chebyshev wavelets [37] and Gegenbauer wavelets [38], and some of the continuous orthonormal polynomial wavelets [39, 40].

The current work's objective is to create a Fibonacci wavelets collocation method that is fast and simple. It guarantees the required accuracy for a relatively small number of grid points to solve the SFDEs. It is challenging to find the necessary approximations using a new numerical design. A recent addition to the family of wavelets is the Fibonacci wavelets formed by Fibonacci polynomials. Due to its superior properties and advantages over other wavelets, it grabs the attention of many researchers.

As a consequence, researchers start using this package to solve mathematical problems such as time-fractional telegraph equation [41], hyperbolic partial differential equations [42], time-varying delay problems [43], fractional Rosenau–Hyman equations [44], time-fractional bioheat transfer model [45], dispersive partial differential equation [46], spectral solution of FDEs [47], nonlinear Hunter–Saxton Equation [32], nonlinear stratonovich Volterra integral equations [48]. Some of the articles utilized to improve the quality of the paper such as fractional stochastic integro-differential equation by B-spline functions [49], the construction of operational matrix of fractional derivatives using B-spline functions [50], Fokker–Planck equation using the flatlet oblique multiwavelets [51], and fractional convection–diffusion equation using the flatlet oblique multiwavelets [52]. Here, the Fibonacci wavelet collocation technique was successfully applied to the model, and significant approximation was obtained in the model's solution. To our knowledge, no one has solved this system of FDEs by Fibonacci wavelets, which motivates us to study this by the developed strategy. The absolute error with the Exact solution and ND Solver solution for various values of M and k are computed to demonstrate the efficacy and accuracy of the developed strategy. Standard wavelets such as Haar wavelet and Daubechies wavelets satisfy

the MRA conditions. Here, we considered Fibonacci wavelets generated by using Fibonacci polynomials. Due to this, it doesn't satisfy the MRA, which is valid for standard wavelets.

The structure of this article is as follows: Sect. 2, named "Preliminaries," provides the definitions of wavelets. OMI of Fibonacci wavelets carried out in Sect. 3. The method of solution and application of the proposed scheme is explained in Sects. 4 and 5, respectively. Finally, Sect. 6 gives the conclusion of the article.

2 Preliminaries

Definition 1: Riemann–Liouville fractional derivative The Riemann–Liouville integral operator of order α is defined by [43]:

$$(I^\alpha u)(\zeta) = \begin{cases} \frac{1}{\Gamma(\alpha)} \int_0^\zeta (\zeta - t)^\alpha u(t) dt, & \alpha > 0, t > 0, \\ u(t) & \alpha = 0, \end{cases}$$

And its fractional derivative order $\alpha (\alpha \geq 0)$ is typically used:

$$(D^\alpha u)(\zeta) = \left(\frac{d}{dt}\right)^n (I^{n-\alpha} u)(\zeta), \quad \alpha > 0, n - 1 < \alpha \leq n.$$

Definition 2 [53]: Multiresolution analysis (MRA) A multiresolution analysis for $L^2(\mathbb{R})$ consists of a sequence of closed subspaces $\{V_j\}_{j \in \mathbb{Z}}$ of $L^2(\mathbb{R})$ and a function $\phi \in V_0$, such that the following conditions hold:

- i. The spaces V_j are nested, i.e., $\dots V_{-1} \subset V_0 \subset V_1 \dots$.
- ii. $\overline{\bigcup_{j \in \mathbb{Z}} V_j} = L^2(\mathbb{R})$ and $\bigcap_{j \in \mathbb{Z}} V_j = \{0\}$.
- iii. For all $j \in \mathbb{Z}, V_{j+1} = D(V_j)$.
- iv. $f \in V_0 \Rightarrow T_k f \in V_0, \forall k \in \mathbb{Z}$.
- v. $\{T_k \phi\}_{k \in \mathbb{Z}}$ is an orthogonal basis for V_0 .

Definition 3: Fibonacci wavelets On the interval $[0, 1]$, the Fibonacci wavelets are defined as [43],

$$\vartheta_{n,m}(\zeta) = \begin{cases} \frac{2^{\frac{k-1}{2}}}{\sqrt{w_m}} P_m(2^{k-1} \zeta - \hat{n}), & \frac{\hat{n}}{2^{k-1}} \leq \zeta < \frac{\hat{n}+1}{2^{k-1}} \\ 0, & \text{Otherwise,} \end{cases}$$

with

$$w_m = \int_0^1 (P_m(\zeta))^2 d\zeta,$$

where $P_m(\zeta)$ is the Fibonacci polynomial of degree- m , translation parameter $n = 1, 2, \dots, 2^{k-1}$ and, k represents the level of resolution $k = 1, 2, \dots$ and respectively. The quantity $\frac{1}{\sqrt{w_m}}$ is a normalization factor. The Fibonacci polynomials are defined as follows in the form of the recurrence relation for every $\zeta \in R^+$:

$$P_{m+2}(\zeta) = \zeta P_{m+1}(\zeta) + P_m(\zeta), \quad \forall m \geq 0,$$

with initial conditions $P_0(\zeta) = 1, P_1(\zeta) = \zeta$. These polynomials can also be defined using the succeeding universal formula:

$$P_m(\zeta) = \begin{cases} 1, & m = 0, \\ \zeta, & m = 1, \\ \zeta P_{m-1}(\zeta) + P_{m-2}(\zeta), & m > 1, \end{cases}$$

Fibonacci wavelets are compactly supported wavelets formed by Fibonacci polynomials over the interval $[0, 1]$.

Theorem 1 [31] *Let $L^2[0, 1]$ be the Hilbert space generated by the Fibonacci wavelet basis. Let $\eta(\zeta)$ be the continuous bounded function in $L^2[0, 1]$. Then, the Fibonacci wavelet expansion of $\eta(\zeta)$ converges with it.*

Proof Let $\eta : [0, 1] \rightarrow R$ be a continuous function and $|\eta(\zeta)| \leq \mu$, where μ is any real number. Then, Fibonacci wavelet approximation of $\eta(\zeta)$ can be expressed as,

$$\eta(\zeta) = \sum_{n=1}^{2^{\frac{k-1}{2}}} \sum_{m=0}^{M-1} a_{n,m} \vartheta_{n,m}(\zeta),$$

$$a_{n,m} = \langle \eta(\zeta), \vartheta_{n,m}(\zeta) \rangle$$

denotes inner product.

$$a_{n,m} = \int_0^1 \eta(\zeta) \vartheta_{n,m}(\zeta) d\zeta,$$

$$a_{n,m} = \int_I \eta(\zeta) \frac{2^{\frac{k-1}{2}}}{\sqrt{w_m}} P_m(2^{k-1}\zeta - n + 1) d\zeta,$$

where $I = \left[\frac{n-1}{2^{k-1}}, \frac{n}{2^{k-1}} \right)$

Then substitute $2^{k-1}\zeta - n + 1 = y$ then we get,

$$a_{n,m} = \frac{2^{\frac{k-1}{2}}}{\sqrt{w_m}} \int_0^1 \eta\left(\frac{y+n-1}{2^{k-1}}\right) P_m(y) \frac{dy}{2^{k-1}}$$

$$a_{n,m} = \frac{2^{\frac{-k+1}{2}}}{\sqrt{w_m}} \int_0^1 \eta\left(\frac{y+n-1}{2^{k-1}}\right) P_m(y) dy$$

By generalized mean value theorem,

$$a_{n,m} = \frac{2^{\frac{-k+1}{2}}}{\sqrt{w_m}} \eta\left(\frac{x+n-1}{2^{k-1}}\right) \int_0^1 P_m(y) dy \quad \text{for some } x \in (0, 1)$$

Since $P_m(y)$ is a bounded continuous function. Put $\int_0^1 P_m(y) dy = h$

$$|a_{n,m}| = \left| \frac{2^{\frac{-k+1}{2}}}{\sqrt{w_m}} \left| \eta\left(\frac{x+n-1}{2^{k-1}}\right) \right| h \right|$$

Since η remains bounded

$$\text{Hence, } |a_{n,m}| \leq \left| \frac{2^{\frac{-k+1}{2}} \mu h}{\sqrt{w_m}} \right|$$

Therefore, $\sum_{n,m=0}^{\infty} a_{n,m}$ is absolutely convergent. Hence, the Fibonacci wavelet series expansion $\eta(\zeta)$ converges uniformly to it.

Theorem 2 [54] *Let $I \subset R$ be a finite interval with length $m(I)$. Furthermore, $f(\zeta)$ is an integrable function defined on I and $\sum_{i=0}^{M-1} \sum_{j=1}^{2^{k-1}} a_{i,j} \vartheta_{i,j}(\zeta)$ be a good Fibonacci wave-*

let approximation of f on I with for some $\epsilon > 0$, $\left| f(\zeta) - \sum_{i=0}^{M-1} \sum_{j=1}^{2^{k-1}} a_{i,j} \vartheta_{i,j}(\zeta) \right| \leq \epsilon, \forall x \in I$.

Then $-\epsilon m(I) + \int_I \sum \sum a_{i,j} \vartheta_{i,j}(\zeta) d\zeta \leq \int_I f(\zeta) d\zeta \leq \epsilon m(I) + \int_I \sum \sum a_{i,j} \vartheta_{i,j}(\zeta) d\zeta$.

This theorem says that when an integral of a complicated function is not possible, it can be evaluated by approximately the $f(\zeta)$ by wavelet functions in a given interval.

3 Functional matrix of integration (FMI)

At $k = 1$ and $M = 6$, In [42], the author generated the Fibonacci wavelet basis and obtained the functional matrix as below:

$$\vartheta_{1,0}(\zeta) = 1$$

$$\vartheta_{1,1}(\zeta) = \sqrt{3}\zeta$$

$$\vartheta_{1,2}(\zeta) = \frac{1}{2} \sqrt{\frac{15}{7}} (1 + \zeta^2)$$

$$\vartheta_{1,3}(\zeta) = \sqrt{\frac{105}{239}} \zeta (2 + \zeta^2)$$

$$\vartheta_{1,4}(\zeta) = 3 \sqrt{\frac{35}{1943}} (1 + 3\zeta^2 + \zeta^4)$$

$$\vartheta_{1,5}(\zeta) = \frac{3}{4} \sqrt{\frac{385}{2582}} \zeta (3 + 4\zeta^2 + \zeta^4)$$

$$\vartheta_{1,6}(\zeta) = 3 \sqrt{\frac{5005}{1268209}} (1 + 6\zeta^2 + 5\zeta^4 + \zeta^6)$$

$$\vartheta_{1,7}(\zeta) = 3 \sqrt{\frac{5005}{2827883}} \zeta (4 + 10\zeta^2 + 6\zeta^4 + \zeta^6)$$

Integrating the above first six bases concerning ζ limit from 0 to ζ , and the Fibonacci wavelet bases are then expressed as a linear combination as;

$$\int_0^{\zeta} \vartheta_{1,0}(\zeta) d\zeta = \left[0 \quad \frac{1}{\sqrt{3}} \quad 0 \quad 0 \quad 0 \quad 0 \right] \vartheta_6(\zeta)$$

$$\int_0^{\zeta} \vartheta_{1,1}(\zeta) d\zeta = \left[-\frac{\sqrt{3}}{2} \quad 0 \quad \sqrt{\frac{7}{5}} \quad 0 \quad 0 \quad 0 \right] \vartheta_6(\zeta)$$

$$\int_0^{\zeta} \vartheta_{1,2}(\zeta) d\zeta = \left[0 \quad \frac{\sqrt{5}}{6\sqrt{7}} \quad 0 \quad \frac{\sqrt{239}}{42} \quad 0 \quad 0 \right] \vartheta_6(\zeta)$$

$$\int_0^{\zeta} \vartheta_{1,3}(\zeta) d\zeta = \left[-\frac{\sqrt{105}}{2\sqrt{239}} \quad 0 \quad \frac{7}{2\sqrt{239}} \quad 0 \quad \frac{\sqrt{1943}}{4\sqrt{717}} \quad 0 \right] \vartheta_6(\zeta)$$

$$\int_0^{\zeta} \vartheta_{1,4}(\zeta) d\zeta = \left[0 \quad 0 \quad 0 \quad \frac{\sqrt{717}}{5\sqrt{1943}} \quad 0 \quad \frac{4\sqrt{2582}}{5\sqrt{21373}} \right] \vartheta_6(\zeta)$$

$$\int_0^\xi \vartheta_{1,5}(\zeta) d\zeta = \left[-\frac{\sqrt{385}}{4\sqrt{2582}} \quad 0 \quad 0 \quad 0 \quad \frac{\sqrt{21373}}{24\sqrt{2582}} \quad 0 \right] \vartheta_6(\zeta)$$

$$\int_0^\xi \vartheta(\zeta) d\zeta = \mathbb{B}_{6 \times 6} \vartheta_6(\zeta) + \overline{\vartheta_6(\zeta)} \tag{3}$$

where

$$\vartheta_6(\zeta) = [\vartheta_{1,0}(\zeta), \vartheta_{1,1}(\zeta), \vartheta_{1,2}(\zeta), \vartheta_{1,3}(\zeta), \vartheta_{1,4}(\zeta), \vartheta_{1,5}(\zeta)]^T$$

$$\mathbb{B}_{6 \times 6} = \begin{bmatrix} 0 & \frac{1}{\sqrt{3}} & 0 & 0 & 0 & 0 \\ -\frac{\sqrt{3}}{2} & 0 & \sqrt{\frac{7}{5}} & 0 & 0 & 0 \\ 0 & \frac{\sqrt{5}}{6\sqrt{7}} & 0 & \frac{\sqrt{239}}{42} & 0 & 0 \\ -\frac{\sqrt{105}}{2\sqrt{239}} & 0 & \frac{7}{2\sqrt{239}} & 0 & \frac{\sqrt{1943}}{4\sqrt{717}} & 0 \\ 0 & 0 & 0 & \frac{\sqrt{717}}{5\sqrt{1943}} & 0 & \frac{4\sqrt{2582}}{5\sqrt{21373}} \\ -\frac{\sqrt{385}}{4\sqrt{2582}} & 0 & 0 & 0 & \frac{\sqrt{21373}}{24\sqrt{2582}} & 0 \end{bmatrix}, \quad \overline{\vartheta_6(\zeta)} = \begin{bmatrix} 0 \\ 0 \\ 0 \\ 0 \\ \frac{\sqrt{1268209}}{24\sqrt{33566}} \vartheta_{1,6}(\zeta) \end{bmatrix}$$

Integrating the aforementioned basis again, we arrive at the following:

$$\int_0^\xi \int_0^\xi \vartheta_{1,0}(\zeta) d\zeta = \left[-\frac{1}{2} \quad 0 \quad \sqrt{\frac{7}{15}} \quad 0 \quad 0 \quad 0 \right] \vartheta_6(\zeta),$$

$$\int_0^\xi \int_0^\xi \vartheta_{1,1}(\zeta) d\zeta = \left[0 \quad -\frac{1}{3} \quad 0 \quad \frac{\sqrt{239}}{6\sqrt{35}} \quad 0 \quad 0 \right] \vartheta_6(\zeta),$$

$$\int_0^\xi \int_0^\xi \vartheta_{1,2}(\zeta) d\zeta = \left[-\frac{\sqrt{5}}{2\sqrt{21}} \quad 0 \quad \frac{1}{4} \quad 0 \quad \frac{\sqrt{1943}}{168\sqrt{3}} \quad 0 \right] \vartheta_6(\zeta),$$

$$\int_0^\xi \int_0^\xi \vartheta_{1,3}(\zeta) d\zeta = \left[0 \quad -\frac{5\sqrt{35}}{12\sqrt{239}} \quad 0 \quad \frac{2}{15} \quad 0 \quad \frac{\sqrt{2582}}{5\sqrt{7887}} \right] \vartheta_6(\zeta),$$

$$\int_0^\zeta \int_0^\zeta \vartheta_{1,4}(\zeta) d\zeta = \begin{bmatrix} -\frac{\sqrt{35}}{2\sqrt{1943}} & 0 & \frac{7\sqrt{3}}{10\sqrt{1943}} & 0 & \frac{1}{12} & 0 \end{bmatrix} \vartheta_6(\zeta),$$

$$\int_0^\zeta \int_0^\zeta \vartheta_{1,5}(\zeta) d\zeta = \begin{bmatrix} 0 & -\frac{\sqrt{385}}{4\sqrt{7746}} & 0 & \frac{\sqrt{2629}}{40\sqrt{7746}} & 0 & \frac{2}{35} \end{bmatrix} \vartheta_6(\zeta),$$

Hence,

$$\int_0^\zeta \int_0^\zeta \vartheta(\zeta) d\zeta = \mathbb{B}'_{6 \times 6} \vartheta_6(\zeta) + \overline{\vartheta}'_6(\zeta) \quad (4)$$

where

$$\mathbb{B}'_{6 \times 6} = \begin{bmatrix} -\frac{1}{2} & 0 & \sqrt{\frac{7}{15}} & 0 & 0 & 0 \\ 0 & -\frac{1}{3} & 0 & \frac{\sqrt{239}}{6\sqrt{35}} & 0 & 0 \\ -\frac{\sqrt{5}}{2\sqrt{21}} & 0 & \frac{1}{4} & 0 & \frac{\sqrt{1943}}{168\sqrt{3}} & 0 \\ 0 & -\frac{5\sqrt{35}}{12\sqrt{239}} & 0 & \frac{2}{15} & 0 & \frac{\sqrt{2582}}{5\sqrt{7887}} \\ -\frac{\sqrt{35}}{2\sqrt{1943}} & 0 & \frac{7\sqrt{3}}{10\sqrt{1943}} & 0 & \frac{1}{12} & 0 \\ 0 & -\frac{\sqrt{385}}{4\sqrt{7746}} & 0 & \frac{\sqrt{2629}}{40\sqrt{7746}} & 0 & \frac{2}{35} \\ -\frac{\sqrt{5005}}{4\sqrt{1268209}} & 0 & 0 & 0 & \frac{\sqrt{277849}}{42\sqrt{1268209}} & 0 \\ 0 & -\frac{\sqrt{15015}}{4\sqrt{2827883}} & 0 & 0 & 0 & \frac{\sqrt{16783}}{7\sqrt{5655766}} \\ -\frac{3\sqrt{17017}}{8\sqrt{140977105}} & 0 & 0 & 0 & 0 & 0 \\ 0 & -\sqrt{\frac{969969}{25081424945}} & 0 & 0 & 0 & 0 \end{bmatrix}, \quad \overline{\vartheta}'_6(\zeta) = \begin{bmatrix} 0 \\ 0 \\ 0 \\ 0 \\ \frac{\sqrt{1268209}}{\sqrt{277849}} \vartheta_{1,6}(\zeta) \\ \frac{30}{\sqrt{2827883}} \vartheta_{1,7}(\zeta) \\ \frac{168}{33566} \vartheta_{1,7}(\zeta) \end{bmatrix}$$

The Fibonacci wavelet basis is examined at $k=2$ and $M=6$ as follows:

$$\left. \begin{aligned} \vartheta_{1,0}(\zeta) &= \sqrt{2} \\ \vartheta_{1,1}(\zeta) &= 2\sqrt{6}\zeta \\ \vartheta_{1,2}(\zeta) &= \sqrt{\frac{15}{14}}(1 + 4\zeta^2) \\ \vartheta_{1,3}(\zeta) &= 4\sqrt{\frac{210}{239}}(\zeta + 2\zeta^3) \\ \vartheta_{1,4}(\zeta) &= 3\sqrt{\frac{70}{1943}}(1 + 12\zeta^2 + 16\zeta^4) \\ \vartheta_{1,5}(\zeta) &= \frac{3}{2}\sqrt{\frac{385}{1291}}\zeta(3 + 16\zeta^2 + 16\zeta^4) \end{aligned} \right\} 0 \leq \zeta < \frac{1}{2}$$

$$\left. \begin{aligned} \vartheta_{2,0}(\zeta) &= \sqrt{2} \\ \vartheta_{2,1}(\zeta) &= \sqrt{6}(-1 + 2\zeta) \\ \vartheta_{2,2}(\zeta) &= \sqrt{\frac{30}{7}}(1 - 2\zeta + 2\zeta^2) \\ \vartheta_{2,3}(\zeta) &= \sqrt{\frac{210}{239}}(-1 + 2\zeta)(3 - 4\zeta + 4\zeta^2) \\ \vartheta_{2,4}(\zeta) &= 3\sqrt{\frac{70}{1943}}(5 - 20\zeta + 36\zeta^2 - 32\zeta^3 + 16\zeta^4) \\ \vartheta_{2,5}(\zeta) &= 6\sqrt{\frac{385}{1291}}(-1 + 2\zeta)(1 - 3\zeta + 5\zeta^2 - 4\zeta^3 + 2\zeta^4) \end{aligned} \right\} \frac{1}{2} \leq \zeta < 1$$

$$\int_0^\zeta \vartheta(\zeta) d\zeta = \mathbb{B}_{12 \times 12} \vartheta_{12}(\zeta) + \overline{\vartheta_{12}(\zeta)}, \tag{5}$$

where $\vartheta_{12}(\zeta) = [\vartheta_{1,0}(\zeta), \vartheta_{1,1}(\zeta), \vartheta_{1,2}(\zeta), \vartheta_{1,3}(\zeta), \vartheta_{1,4}(\zeta), \vartheta_{1,5}(\zeta), \vartheta_{2,0}(\zeta), \vartheta_{2,1}(\zeta), \vartheta_{2,2}(\zeta), \vartheta_{2,3}(\zeta), \vartheta_{2,4}(\zeta), \vartheta_{2,5}(\zeta)]^T$,

$$\mathbb{B}_{12 \times 12} = \begin{bmatrix} 0 & \frac{1}{2\sqrt{3}} & 0 & 0 & 0 & 0 & 0 & 0 & 0 & 0 & 0 & 0 \\ -\frac{\sqrt{3}}{4} & 0 & \frac{\sqrt{7}}{2} & 0 & 0 & 0 & 0 & 0 & 0 & 0 & 0 & 0 \\ 0 & \frac{\sqrt{5}}{12\sqrt{7}} & 0 & \frac{\sqrt{239}}{84} & 0 & 0 & 0 & 0 & 0 & 0 & 0 & 0 \\ -\frac{\sqrt{105}}{4\sqrt{239}} & 0 & \frac{7}{4\sqrt{239}} & 0 & \frac{\sqrt{1943}}{8\sqrt{717}} & 0 & 0 & 0 & 0 & 0 & 0 & 0 \\ 0 & 0 & 0 & \frac{\sqrt{717}}{10\sqrt{1943}} & 0 & \frac{2\sqrt{2582}}{5\sqrt{21373}} & 0 & 0 & 0 & 0 & 0 & 0 \\ -\frac{\sqrt{385}}{8\sqrt{2582}} & 0 & 0 & 0 & \frac{\sqrt{21373}}{48\sqrt{2582}} & 0 & 0 & 0 & 0 & 0 & 0 & 0 \\ 0 & 0 & 0 & 0 & 0 & 0 & 0 & \frac{1}{2\sqrt{3}} & 0 & 0 & 0 & 0 \\ 0 & 0 & 0 & 0 & 0 & 0 & -\frac{\sqrt{3}}{4} & 0 & \frac{\sqrt{7}}{2} & 0 & 0 & 0 \\ 0 & 0 & 0 & 0 & 0 & 0 & 0 & \frac{\sqrt{5}}{12\sqrt{7}} & 0 & \frac{\sqrt{239}}{84} & 0 & 0 \\ 0 & 0 & 0 & 0 & 0 & 0 & -\frac{\sqrt{105}}{4\sqrt{239}} & 0 & 0 & 0 & \frac{\sqrt{21373}}{48\sqrt{2582}} & 0 \\ 0 & 0 & 0 & 0 & 0 & 0 & 0 & 0 & 0 & 0 & \frac{\sqrt{717}}{10\sqrt{1943}} & 0 \\ 0 & 0 & 0 & 0 & 0 & 0 & -\frac{\sqrt{385}}{8\sqrt{2582}} & 0 & 0 & 0 & \frac{\sqrt{21373}}{48\sqrt{2582}} & 0 \end{bmatrix}, \overline{\vartheta_{12}(\zeta)} = \begin{bmatrix} 0 \\ 0 \\ 0 \\ 0 \\ 0 \\ \frac{\sqrt{1268209}}{\sqrt{33566}} \vartheta_{1,6}(\zeta) \\ 0 \\ 0 \\ 0 \\ 0 \\ \frac{\sqrt{1268209}}{\sqrt{33566}} \vartheta_{2,6}(\zeta) \\ 0 \end{bmatrix}$$

Similarly, the second integration can be written as:

$$\int_0^\zeta \int_0^\zeta \vartheta(\zeta) d\zeta d\zeta = \mathbb{B}'_{12 \times 12} \vartheta_{12}(\zeta) + \overline{\vartheta'_{12}(\zeta)} \tag{6}$$

w h e r e $\vartheta_{12}(\zeta) = [\vartheta_{1,0}(\zeta), \vartheta_{1,1}(\zeta), \vartheta_{1,2}(\zeta), \vartheta_{1,3}(\zeta), \vartheta_{1,4}(\zeta), \vartheta_{1,5}(\zeta), \vartheta_{2,0}(\zeta), \vartheta_{2,1}(\zeta), \vartheta_{2,2}(\zeta), \vartheta_{2,3}(\zeta), \vartheta_{2,4}(\zeta), \vartheta_{2,5}(\zeta)]^T$,

$$B'_{12 \times 12} = \begin{pmatrix} -\frac{1}{8} & 0 & \frac{\sqrt{7}}{4} & 0 & 0 & 0 & 0 & 0 & 0 & 0 & 0 & 0 \\ 0 & -\frac{1}{12} & 0 & \frac{\sqrt{239}}{24} & 0 & 0 & 0 & 0 & 0 & 0 & 0 & 0 \\ -\frac{\sqrt{21}}{8} & 0 & \frac{1}{16} & 0 & \frac{\sqrt{1945}}{672} & 0 & 0 & 0 & 0 & 0 & 0 & 0 \\ 0 & \frac{5\sqrt{35}}{\sqrt{2744}} & 0 & \frac{1}{30} & 0 & \frac{\sqrt{1291}}{10} & 0 & 0 & 0 & 0 & 0 & 0 \\ -\frac{\sqrt{35}}{\sqrt{1945}} & 0 & \frac{7\sqrt{3}}{\sqrt{1945}} & 0 & \frac{1}{48} & 0 & 0 & 0 & 0 & 0 & 0 & 0 \\ 0 & -\frac{\sqrt{385}}{\sqrt{7745}} & 0 & \frac{\sqrt{2629}}{\sqrt{7745}} & 0 & \frac{1}{70} & 0 & 0 & 0 & 0 & 0 & 0 \\ 0 & 0 & 0 & 0 & 0 & 0 & -\frac{1}{8} & 0 & \frac{\sqrt{7}}{4} & 0 & 0 & 0 \\ 0 & 0 & 0 & 0 & 0 & 0 & 0 & -\frac{1}{12} & 0 & \frac{\sqrt{239}}{24} & 0 & 0 \\ 0 & 0 & 0 & 0 & 0 & 0 & -\frac{\sqrt{5}}{8} & 0 & \frac{1}{16} & 0 & \frac{\sqrt{1945}}{672} & 0 \\ 0 & 0 & 0 & 0 & 0 & 0 & \frac{5\sqrt{35}}{\sqrt{2744}} & 0 & \frac{1}{30} & 0 & \frac{\sqrt{1291}}{10} & 0 \\ 0 & 0 & 0 & 0 & 0 & 0 & -\frac{\sqrt{35}}{\sqrt{1945}} & 0 & \frac{7\sqrt{3}}{\sqrt{1945}} & 0 & \frac{1}{48} & 0 \\ 0 & 0 & 0 & 0 & 0 & 0 & -\frac{\sqrt{385}}{\sqrt{7745}} & 0 & \frac{\sqrt{2629}}{\sqrt{7745}} & 0 & \frac{1}{70} & 0 \end{pmatrix}, \vartheta'_{12}(\zeta) = \begin{pmatrix} 0 \\ 0 \\ 0 \\ 0 \\ \frac{\sqrt{1268209}}{\sqrt{277849}} \vartheta_{1,6}(\zeta) \\ \frac{120}{\sqrt{33566}} \vartheta_{1,7}(\zeta) \\ 0 \\ 0 \\ 0 \\ 0 \\ \frac{\sqrt{1268209}}{\sqrt{277849}} \vartheta_{2,6}(\zeta) \\ \frac{120}{\sqrt{33566}} \vartheta_{2,7}(\zeta) \\ 0 \\ 0 \end{pmatrix}$$

Similarly, we can make matrices for our convenience.

4 Fibonacci wavelet method

In this part, the Fibonacci wavelet collocation method (FWCM) is used to solve a Brusselator model in the form of a system of coupled fractional order differential equations numerically. Consider the following nonlinear fractional-order Brusselator system of two equations of the state:

$$\left. \begin{aligned} D^\alpha Y_1(\zeta) &= \lambda - (\delta + 1)Y_1(\zeta) + Y_2^2(\zeta) Y_1(\zeta) \\ D^\beta Y_2(\zeta) &= \delta Y_1(\zeta) - Y_2^2(\zeta) Y_1(\zeta) \end{aligned} \right\} \zeta \in [0, 1] \tag{7}$$

With the initial conditions of the above system, given by $Y_1(0) = u_0, Y_2(0) = v_0$. Assume that,

$$\left. \begin{aligned} \frac{dY_1(\zeta)}{d\zeta} &= A^T \vartheta(\zeta) \\ \frac{dY_2(\zeta)}{d\zeta} &= B^T \vartheta(\zeta) \end{aligned} \right\} \tag{8}$$

where

$$A^T = [a_{1,0}, \dots, a_{1,M-1}, a_{2,0}, \dots, a_{2,M-1}, a_{2^{k-1},0}, \dots, a_{2^{k-1},M-1}],$$

$$B^T = [b_{1,0}, \dots, b_{1,M-1}, b_{2,0}, \dots, b_{2,M-1}, b_{2^{k-1},0}, \dots, b_{2^{k-1},M-1}],$$

$$\vartheta(\zeta) = [\vartheta(\zeta)_{1,0}, \dots, \vartheta(\zeta)_{1,M-1}, \vartheta(\zeta)_{2,0}, \dots, \vartheta(\zeta)_{2,M-1}, \vartheta(\zeta)_{2^{k-1},0}, \dots, \vartheta(\zeta)_{2^{k-1},M-1}].$$

Integrating Eq. (8) concerning ‘ ζ ’ from ‘0’ to ‘ ζ ’. We get

$$Y_1(\zeta) = Y_1(0) + \int_0^\zeta A^T \vartheta(\zeta) d\zeta$$

$$Y_2(\zeta) = Y_2(0) + \int_0^\zeta B^T \vartheta(\zeta) d\zeta$$

Using Eq. (3) and initial conditions expressed in terms of $\vartheta(\zeta)$. we obtain

$$\left. \begin{aligned} Y_1(\zeta) &= C^T \vartheta(\zeta) + A^T [\mathbb{B} \vartheta(\zeta) + \overline{\vartheta}(\zeta)] \\ Y_2(\zeta) &= E^T \vartheta(\zeta) + B^T [\mathbb{B} \vartheta(\zeta) + \overline{\vartheta}(\zeta)] \end{aligned} \right\} \tag{9}$$

where C and E are the known vectors. Differentiate (9) fractionally concerning ζ using the Riemann–Liouville derivative definition. Then, we get

$$\left. \begin{aligned} D_\zeta^\alpha Y_1(\zeta) &= D_\zeta^\alpha (C^T \vartheta(\zeta) + A^T [\mathbb{B} \vartheta(\zeta) + \overline{\vartheta}(\zeta)]) \\ D_\zeta^\beta Y_2(\zeta) &= D_\zeta^\beta (E^T \vartheta(\zeta) + B^T [\mathbb{B} \vartheta(\zeta) + \overline{\vartheta}(\zeta)]) \end{aligned} \right\} \tag{10}$$

Now, substitute (9) and (10) in (7) and collocate the obtained equations by the following collocation points $\zeta_i = \frac{2i-1}{2^k M}$, $i = 1, 2, \dots, M$ and solve the collocated equations by the Newton–Raphson method, which provides the values of unknown Fibonacci wavelet coefficients. Substitute these coefficient values in (9) yields the FWCM numerical solution for the system (7).

5 Numerical results and discussion

We gave a few examples to demonstrate the method’s applicability and value. All the outcomes are computed using the symbolic calculus programming language Mathematica. In this section, the FWCM-based numerical results are presented.

Example 1 Let’s use the fractional Brusselator system as our first test case by setting $\lambda = 0$ and $\delta = 1$ to get,

$$\left. \begin{aligned} D^\alpha Y_1(\zeta) &= -2Y_1(\zeta) + Y_2^2(\zeta)Y_1(\zeta) \\ D^\beta Y_2(\zeta) &= Y_1(\zeta) - Y_2^2(\zeta)Y_1(\zeta) \end{aligned} \right\} \zeta \in [0, 1] \tag{11}$$

The given initial condition is $Y_1(0) = 1, Y_2(0) = 1$.

For $\alpha = \beta = 1, M = 3,$ and $k = 1,$ the approximate solutions achieved are shown below:

$$Y_1(\zeta) = 1 - 1.041678859020140\zeta + 0.221265254670541\zeta^2 + 0.0690448163116171\zeta^3$$

$$Y_2(\zeta) = 1 + 0.03688408010961130\zeta + 0.321630157827961\zeta^2 - 0.17732230935760\zeta^3$$

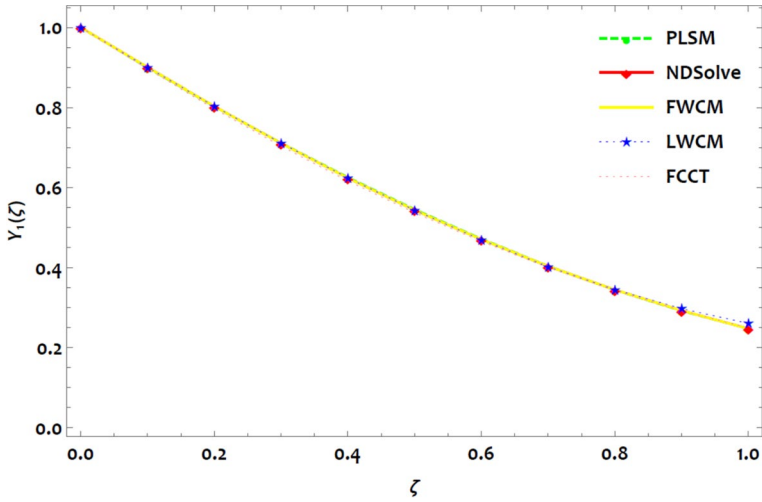


Fig. 1 Comparison of the FWCM solution $Y_1(\zeta)$ graphically with various techniques for Example 1

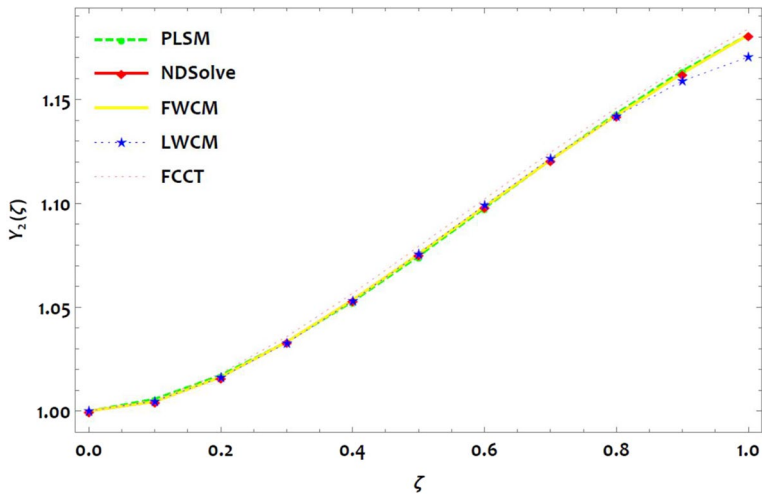


Fig. 2 Comparison of the FWCM solution $Y_2(\zeta)$ graphically with various techniques for Example 1

For $\alpha = \beta = 1$, $M = 6$, and $k = 1$, the approximate solutions achieved are shown below:

$$Y_1(\zeta) = 1 - 1.00038102765750\zeta + 0.0043632799628501\zeta^2 + 0.479058330479812\zeta^3 - 0.32718893005897\zeta^4 + 0.1108247830629921\zeta^5 - 0.0190132308532729\zeta^6$$

Table 1 Numerical comparison of the solution of $Y_1(\zeta)$ with distinct methods for Example 1

| ζ | ND Solve | FWCM | LWCM [12] | PLSM [10] | FCCT [13] |
|---------|-----------------|-----------------|-----------|-------------|---------------|
| 0 | 1.0000000000000 | 1.0000000000000 | 1.0000000 | 1.000000000 | 1.00000000000 |
| 0.1 | 1.0045242287732 | 1.00453411484 | 1.0047829 | 1.005871852 | 1.00538282936 |
| 0.2 | 1.0163740686520 | 1.01638115713 | 1.0162272 | 1.017344916 | 1.01810929129 |
| 0.3 | 1.0333274798201 | 1.03333432101 | 1.0328563 | 1.033338664 | 1.03585318315 |
| 0.4 | 1.0535747927336 | 1.05358233546 | 1.0531936 | 1.052772568 | 1.05671585961 |
| 0.5 | 1.0756500030084 | 1.07565708544 | 1.0757625 | 1.074566121 | 1.07918258244 |
| 0.6 | 1.0983818249491 | 1.09838846827 | 1.0990864 | 1.097638732 | 1.10207887023 |
| 0.7 | 1.1208592873738 | 1.12086648535 | 1.1216887 | 1.120909936 | 1.12452684817 |
| 0.8 | 1.1424036543301 | 1.14241056922 | 1.1420928 | 1.143299184 | 1.14590159775 |
| 0.9 | 1.1625416154948 | 1.16254614587 | 1.1588221 | 1.163725948 | 1.16578750656 |
| 1.0 | 1.1809766803973 | 1.18098843245 | 1.1704000 | 1.181109725 | 1.18393461800 |

Table 2 Numerical comparison of the solution of $Y_2(\zeta)$ with distinct methods available in the literature, for Example 1

| ζ | ND Solve | FWCM | LWCM [12] | PLSM [10] | FCCT [13] |
|---------|-----------------|-----------------|-----------|--------------|----------------|
| 0 | 1.0000000000000 | 1.0000000000000 | 1.0000000 | 1.000000000 | 1.00000000000 |
| 0.1 | 0.9004640068458 | 0.900452958706 | 0.9001627 | 0.8992583774 | 0.896278112238 |
| 0.2 | 0.8034483502329 | 0.803441537107 | 0.8036576 | 0.8029878992 | 0.797037323051 |
| 0.3 | 0.7108240851974 | 0.710818175066 | 0.7113949 | 0.7116391498 | 0.703571118497 |
| 0.4 | 0.6238925384191 | 0.623886377857 | 0.6242848 | 0.6256627136 | 0.616783353382 |
| 0.5 | 0.5435045380585 | 0.543499482082 | 0.5432375 | 0.5455091755 | 0.537234087344 |
| 0.6 | 0.4701498327750 | 0.470145732072 | 0.4691632 | 0.4716291184 | 0.465185420932 |
| 0.7 | 0.4040240619954 | 0.404019666762 | 0.4029721 | 0.4044731282 | 0.400647331682 |
| 0.8 | 0.3450834726110 | 0.345079817029 | 0.3455744 | 0.3444917888 | 0.343423510221 |
| 0.9 | 0.2930932067677 | 0.293092713519 | 0.2978803 | 0.2921356846 | 0.293157196321 |
| 1.0 | 0.2476727083353 | 0.247663204936 | 0.2608000 | 0.2478554632 | 0.249377015000 |

$$Y_2(\zeta) = 1 + 0.00031483757252281\zeta + 0.49657314741236\zeta^2 - 0.48422291674910\zeta^3 + 0.216996981028405\zeta^4 - 0.0587226659136026\zeta^5 + 0.0100490491027540\zeta^6$$

For $\alpha = \beta = 0.25, M = 3$ and $k = 1$, the following approximate solutions are obtained:

$$Y_1(\zeta) = 1 - 3.9967689413279963\zeta + 8.081487786349738\zeta^2 - 4.997760996197616\zeta^3$$

$$Y_2(\zeta) = 1 + 1.074666423156312\zeta - 1.9399866819731517\zeta^2 + 1.1433591270030736\zeta^3$$

For $\alpha = \beta = 0.50, M = 3$ and $k = 1$, the following approximate solutions are obtained:

Table 3 Absolute error (AE) evaluation of the solution of $Y_1(\zeta)$ with diverse values of M and k for Example 1

| ζ | AE of FWCM with ND Solve | | | | k = 1, M = 10 | AE of LWCM with NDSolve | AE of FCCT with NDSolve | AE of PLSM with NDSolve |
|---------|--------------------------|-----------------------|-----------------------|------------------------|-----------------------|-------------------------|-------------------------|-------------------------|
| | k = 1, M = 3, | k = 2, M = 3 | k = 1, M = 6 | k = 2, M = 6 | | | | |
| 0 | 0 | 0 | 0 | 0 | 0 | 0 | 0 | 0 |
| 0.1 | 2.35×10^{-3} | 2.56×10^{-4} | 1.10×10^{-5} | 7.43×10^{-9} | 4.29×10^{-8} | 3.01×10^{-4} | 4.18×10^{-3} | 1.20×10^{-3} |
| 0.2 | 2.38×10^{-3} | 1.06×10^{-4} | 6.81×10^{-6} | 6.68×10^{-8} | 3.13×10^{-8} | 2.09×10^{-4} | 6.18×10^{-3} | 4.60×10^{-4} |
| 0.3 | 1.54×10^{-3} | 9.60×10^{-5} | 5.91×10^{-6} | 2.22×10^{-11} | 2.97×10^{-8} | 5.70×10^{-4} | 7.25×10^{-3} | 8.15×10^{-4} |
| 0.4 | 7.42×10^{-4} | 2.03×10^{-4} | 6.16×10^{-6} | 1.37×10^{-8} | 1.77×10^{-8} | 3.90×10^{-4} | 7.10×10^{-3} | 1.77×10^{-3} |
| 0.5 | 3.97×10^{-4} | 5.05×10^{-6} | 5.05×10^{-6} | 1.97×10^{-8} | 1.97×10^{-8} | 2.67×10^{-4} | 6.27×10^{-3} | 2.00×10^{-3} |
| 0.6 | 5.85×10^{-4} | 8.59×10^{-5} | 4.10×10^{-6} | 2.09×10^{-8} | 1.15×10^{-8} | 9.86×10^{-4} | 4.96×10^{-3} | 1.47×10^{-3} |
| 0.7 | 1.09×10^{-3} | 3.39×10^{-5} | 4.39×10^{-6} | 2.98×10^{-8} | 2.12×10^{-8} | 1.05×10^{-3} | 3.37×10^{-3} | 4.49×10^{-4} |
| 0.8 | 1.46×10^{-3} | 3.00×10^{-5} | 3.65×10^{-6} | 2.32×10^{-8} | 1.57×10^{-8} | 4.90×10^{-4} | 1.65×10^{-3} | 5.91×10^{-4} |
| 0.9 | 1.04×10^{-3} | 6.45×10^{-5} | 4.93×10^{-7} | 2.14×10^{-9} | 3.08×10^{-9} | 4.78×10^{-3} | 6.39×10^{-4} | 9.57×10^{-4} |
| 1.0 | 9.58×10^{-4} | 1.82×10^{-5} | 9.50×10^{-6} | 7.16×10^{-9} | 3.42×10^{-9} | 1.31×10^{-2} | 1.70×10^{-3} | 1.82×10^{-4} |

Table 4 Absolute error (AE) evaluation of the solution of $Y_2(\zeta)$ with diverse values of M and k for Example 1

| ζ | AE of FWCM with ND Solve | | | | k = 1, M = 10 | AE of LWCM with NDSolve | AE of FCCT with NDSolve | AE of PLSM with NDSolve |
|---------|--------------------------|-----------------------|-----------------------|-----------------------|-----------------------|-------------------------|-------------------------|-------------------------|
| | k = 1, M = 3, | k = 2, M = 3 | k = 1, M = 6 | k = 2, M = 6 | | | | |
| 0 | 0 | 0 | 0 | 0 | 0 | 0 | 0 | 0 |
| 0.1 | 2.20×10^{-3} | 2.11×10^{-4} | 9.88×10^{-6} | 4.69×10^{-8} | 5.19×10^{-8} | 2.58×10^{-4} | 8.58×10^{-4} | 1.34×10^{-3} |
| 0.2 | 2.44×10^{-3} | 1.13×10^{-4} | 7.08×10^{-6} | 4.07×10^{-9} | 1.88×10^{-9} | 1.46×10^{-4} | 1.73×10^{-3} | 9.70×10^{-4} |
| 0.3 | 1.89×10^{-3} | 1.11×10^{-5} | 6.84×10^{-6} | 3.86×10^{-8} | 4.50×10^{-8} | 4.71×10^{-4} | 2.52×10^{-3} | 1.11×10^{-5} |
| 0.4 | 1.29×10^{-3} | 2.00×10^{-4} | 7.54×10^{-6} | 2.82×10^{-8} | 3.71×10^{-8} | 3.81×10^{-4} | 3.14×10^{-3} | 8.02×10^{-4} |
| 0.5 | 1.03×10^{-3} | 7.08×10^{-6} | 7.08×10^{-6} | 3.94×10^{-8} | 3.94×10^{-8} | 1.12×10^{-4} | 3.53×10^{-3} | 1.08×10^{-3} |
| 0.6 | 1.23×10^{-4} | 1.06×10^{-4} | 6.64×10^{-6} | 4.49×10^{-9} | 1.30×10^{-8} | 7.04×10^{-4} | 3.69×10^{-3} | 7.43×10^{-4} |
| 0.7 | 1.73×10^{-3} | 5.43×10^{-5} | 7.19×10^{-6} | 7.05×10^{-9} | 1.46×10^{-9} | 8.29×10^{-4} | 3.66×10^{-3} | 5.06×10^{-5} |
| 0.8 | 2.15×10^{-3} | 5.30×10^{-5} | 6.19×10^{-6} | 3.61×10^{-9} | 4.73×10^{-9} | 3.10×10^{-4} | 3.49×10^{-3} | 8.95×10^{-4} |
| 0.9 | 1.90×10^{-3} | 9.81×10^{-5} | 4.53×10^{-6} | 2.29×10^{-8} | 2.99×10^{-8} | 3.71×10^{-3} | 3.24×10^{-4} | 1.18×10^{-3} |
| 1.0 | 2.15×10^{-4} | 8.53×10^{-6} | 1.17×10^{-5} | 3.70×10^{-8} | 5.91×10^{-8} | 1.05×10^{-2} | 2.95×10^{-3} | 1.33×10^{-4} |

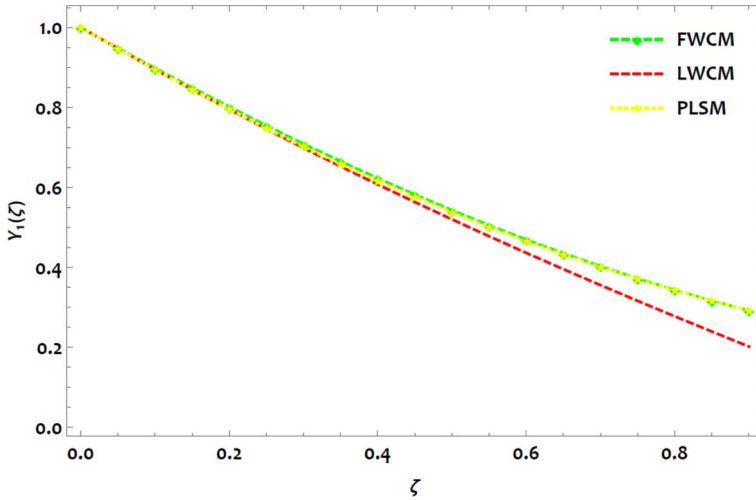


Fig. 3 Graphical comparison of the FWCM solution $Y_1(\zeta)$ at $\alpha = \beta = 0.98$ with different methods of Example 1

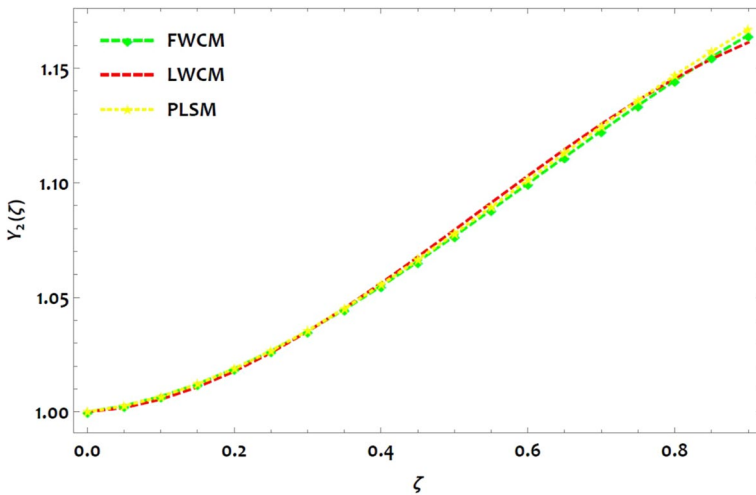


Fig. 4 Graphical comparison of the FWCM solution $Y_2(\zeta)$ at $\alpha = \beta = 0.98$. with different methods of Example 1

$$Y_1(\zeta) = 1 - 2.674387811597822\zeta + 4.161690481082379\zeta^2 - 2.2477452613758127\zeta^3$$

$$Y_2(\zeta) = 1 + 0.520438907294893\zeta - 0.5041694195435757\zeta^2 + 0.2136862725656611\zeta^3$$

Table 5 Comparison of proposed approximate solution for $Y_1(\zeta)$ for different values α and β for the fractional Brussalator model (Example 1)

| ζ | $\alpha = \beta = 0.25$ | $\alpha = \beta = 0.50$ | $\alpha = \beta = 0.75$ | $\alpha = \beta = 0.98$ | | |
|---------|-------------------------|-------------------------|-------------------------|-------------------------|-----------|-------------|
| | FWCM (M=3, k=1) | FWCM (M=3, k=1) | FWCM (M=3, k=1) | FWCM (M=3, k=1) | LWCM [12] | PLSM [10] |
| 0 | 1.00000000000 | 1.00000000000 | 1.00000000000 | 1.00000000000 | 1.0000000 | 1.000000000 |
| 0.1 | 1.08921013462 | 1.04721588281 | 1.02139267322 | 1.00760587309 | 1.0054326 | 1.006641096 |
| 0.2 | 1.14648069037 | 1.08563049486 | 1.04466379274 | 1.02046624576 | 1.0176608 | 1.018844188 |
| 0.3 | 1.17867182223 | 1.11652595379 | 1.06905626761 | 1.03750794327 | 1.0351102 | 1.035502792 |
| 0.4 | 1.19264368428 | 1.14118437724 | 1.09381300688 | 1.05765779087 | 1.0562064 | 1.055510424 |
| 0.5 | 1.19525643196 | 1.16088788283 | 1.11817691965 | 1.07984261384 | 1.0793755 | 1.077760623 |
| 0.6 | 1.19337021982 | 1.17691858822 | 1.14139091483 | 1.10298923744 | 1.1030416 | 1.101146836 |
| 0.7 | 1.19384520265 | 1.19055861102 | 1.16269790161 | 1.12602448692 | 1.1256318 | 1.124562648 |
| 0.8 | 1.20354153509 | 1.20309006888 | 1.18134078942 | 1.14787518757 | 1.1455712 | 1.146901552 |
| 0.9 | 1.22931937203 | 1.21579507944 | 1.19656248606 | 1.16746816462 | 1.1612854 | 1.167057064 |
| 1.0 | 1.27803886819 | 1.22995576032 | 1.20760590183 | 1.18373024336 | 1.1712527 | 1.183922752 |

Table 6 Comparison of proposed approximate solution for $Y_2(\zeta)$ for different values α and β for the fractional Brussalator model (Example 1)

| ζ | $\alpha = \beta = 0.25$ | $\alpha = \beta = 0.50$ | $\alpha = \beta = 0.75$ | $\alpha = \beta = 0.98$ | | |
|---------|-------------------------|-------------------------|-------------------------|-------------------------|-----------|--------------|
| | FWCM (M=3, k=1) | FWCM (M=3, k=1) | FWCM (M=3, k=1) | FWCM (M=3, k=1) | LWCM [12] | PLSM [10] |
| 0 | 1.00000000000 | 1.00000000000 | 1.00000000000 | 1.00000000000 | 1.0000000 | 1.000000000 |
| 0.1 | 0.676140222735 | 0.771930378392 | 0.845594453241 | 0.894584750933 | 0.8947372 | 0.8944807482 |
| 0.2 | 0.483923635219 | 0.613608094833 | 0.719695751352 | 0.795390056942 | 0.7945136 | 0.7953304656 |
| 0.3 | 0.393363671476 | 0.511546677761 | 0.618386094141 | 0.702621402532 | 0.6989464 | 0.7026953614 |
| 0.4 | 0.374473765528 | 0.452259655606 | 0.537747681415 | 0.616484272211 | 0.6076528 | 0.6167216448 |
| 0.5 | 0.397267351399 | 0.422260556856 | 0.473862712982 | 0.537184150486 | 0.5202532 | 0.5375555255 |
| 0.6 | 0.431757863115 | 0.408062909774 | 0.422813388648 | 0.464926521863 | 0.4363552 | 0.4653432112 |
| 0.7 | 0.447958734686 | 0.396180242965 | 0.380681908222 | 0.399916870849 | 0.3555856 | 0.4002309126 |
| 0.8 | 0.415883400148 | 0.373126084794 | 0.343550471509 | 0.342360681951 | 0.2775584 | 0.3423648384 |
| 0.9 | 0.305545293523 | 0.325413963696 | 0.307501278318 | 0.292463439676 | 0.2018908 | 0.2918911978 |
| 1.0 | 0.206957848824 | 0.239557408109 | 0.268616528456 | 0.250430628531 | 0.1282532 | 0.2489562542 |

For $\alpha = \beta = 0.75, M = 3$ and $k = 1,$ the approximate solutions achieved are shown below:

$$Y_1(\zeta) = 1 - 1.6996490259216053\zeta + 1.6212322531648589\zeta^2 - 0.652966698787129\zeta^3$$

$$Y_2(\zeta) = 1 + 0.2020108642640373\zeta + 0.131776862192890\zeta^2 - 0.1261818246293020\zeta^3$$

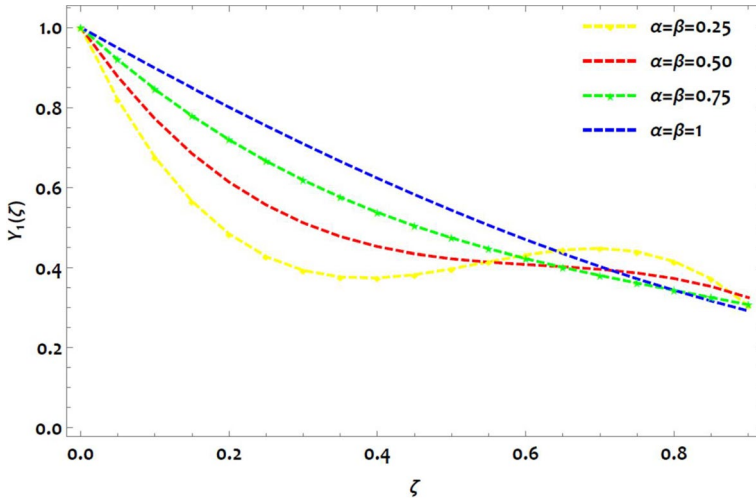


Fig. 5 Approximation of $Y_1(\zeta)$ at distinct values of α and β for Example 1

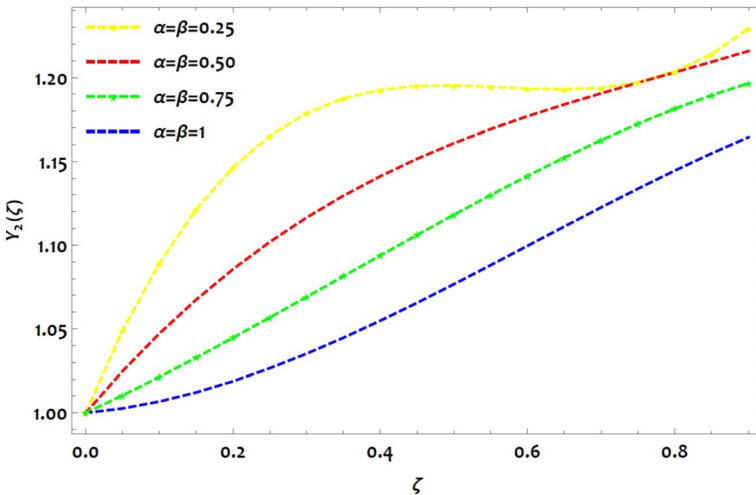


Fig. 6 Approximation of $Y_2(\zeta)$ at distinct values of α and β for Example 1

The FWCM solutions for Example 1 were obtained for the values of $\alpha = \beta = 1$ are shown in Figs. 1 and 2, revealing that the proposed method solutions are reasonably close to the NDSolve results compared to existing methods such as Legendre wavelet collocation method (LWCM), Fractional clique collocation technique (FCCT), Polynomial least square method (PLSM). Numerical approximations obtained by the developed technique (FWCM) and other existing methods are compared with the NDSolve solution (due to the unavailability of the exact solution) are tabulated in Tables 1 and 2, and absolute errors of

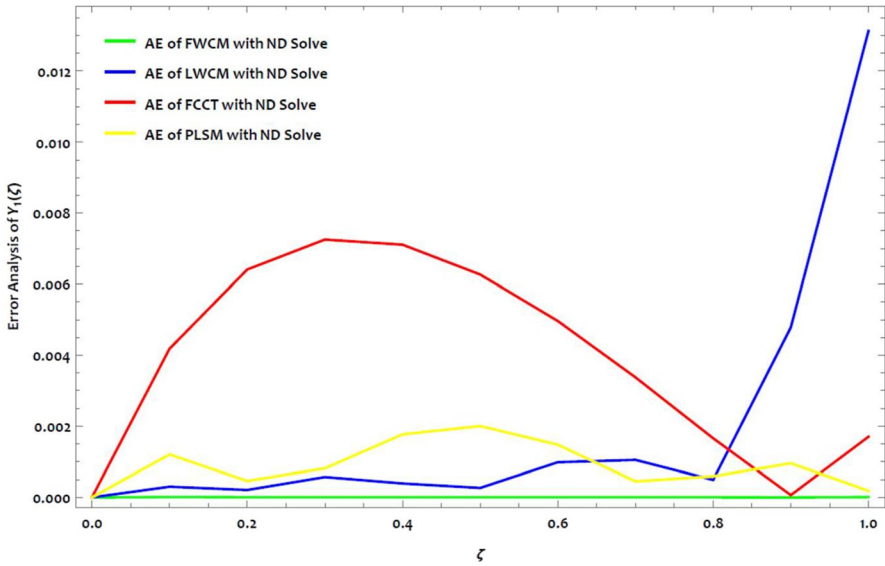


Fig. 7 Visual representation of the Absolute error comparison with different techniques for $Y_1(\zeta)$ of Example 1

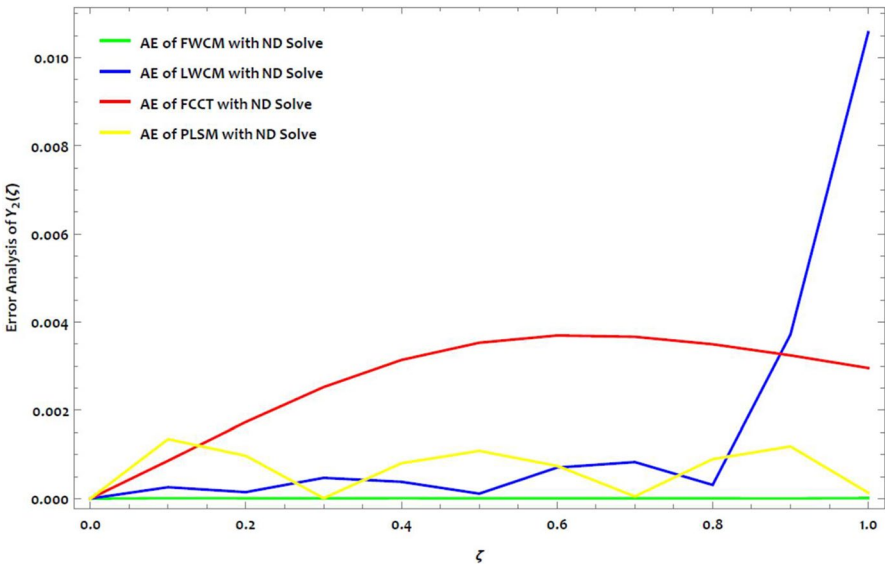


Fig. 8 Visual representation of the Absolute error comparison with different techniques for $Y_2(\zeta)$ of Example 1

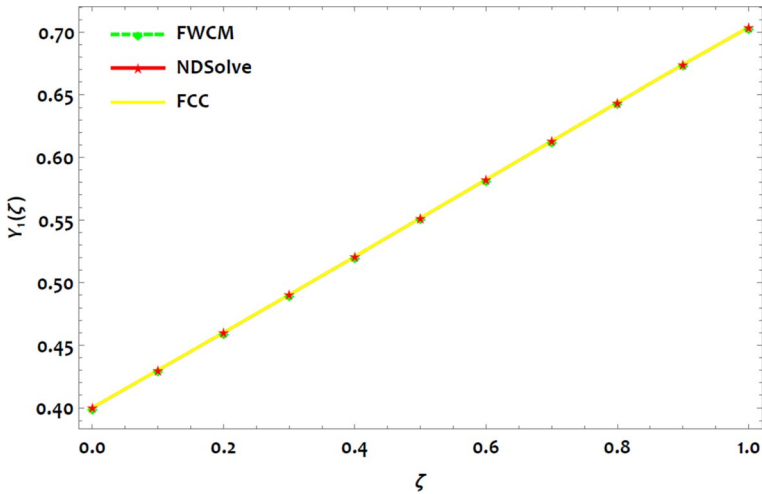


Fig. 9 Graphical comparison of the solution $Y_1(\zeta)$ with different methods of Example 2

the developed approach with the NDSolve solution are tabulated in Tables 3 and 4. It is easy to see that the errors obtained using the proposed FWCM method are lesser than those obtained using other existing techniques. A comparison of our results to the approximate solutions introduced by LWCM [12], and PLSM [10], when $\alpha = \beta = 0.98$ is displayed in Figs. 3 and 4. The numerical approximation of the model at different values of α and β are computed and listed in Tables 5 and 6. The graphical representation of the solution at $\alpha = \beta = 0.25$, $\alpha = \beta = 0.50$, $\alpha = \beta = 0.75$, and $\alpha = \beta = 1$, respectively drawn on the Figs. 5 and 6. FWCM solutions are calculated at diverse values of M and k . Also, by increasing the values of M and k , we get further precision in the result, which can be seen in Tables 3 and 4. It shows that increasing M and k can obtain a higher-order

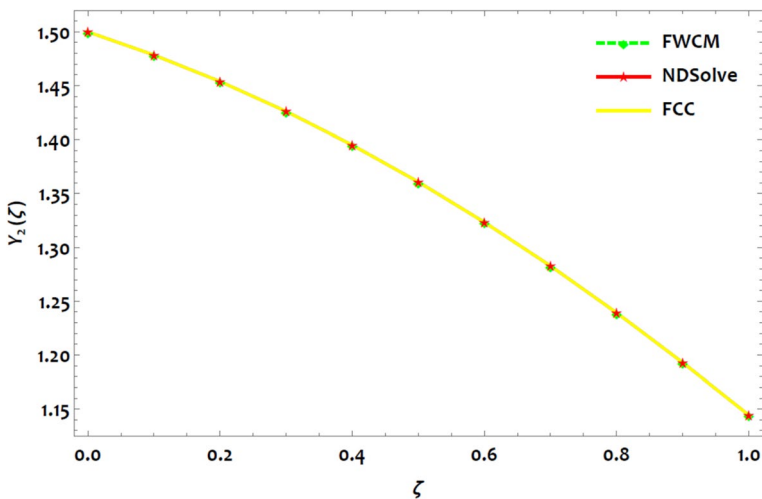


Fig. 10 Graphical comparison of the solution $Y_2(\zeta)$ with different methods of Example 2

Table 7 Absolute error (AE) comparison of the solution of $Y_1(\zeta)$ with different values of M and k for Example 2

| ζ | NDSolve solution | The absolute error of FWCM with NDSolve | | | | AE of FCCT with NDSolve | |
|---------|------------------|---|-----------------------|-----------------------|------------------------|-------------------------|-----------------------|
| | | M=3, k=1 | | M=6, k=2 | | | |
| | | M=3, k=1 | M=6, k=1 | M=6, k=2 | M=10, k=1 | | |
| 0 | 0.400000000000 | 0 | 0 | 0 | 0 | 0 | |
| 0.1 | 0.430009597529 | 3.25×10^{-4} | 1.17×10^{-6} | 1.85×10^{-5} | 1.92×10^{-8} | 2.29×10^{-8} | 1.55×10^{-5} |
| 0.2 | 0.460105543237 | 3.61×10^{-4} | 8.17×10^{-7} | 8.60×10^{-6} | 1.50×10^{-8} | 1.90×10^{-8} | 1.81×10^{-5} |
| 0.3 | 0.490361780324 | 2.65×10^{-4} | 7.91×10^{-7} | 8.60×10^{-6} | 1.88×10^{-8} | 2.25×10^{-8} | 1.71×10^{-5} |
| 0.4 | 0.520814230571 | 1.55×10^{-4} | 8.90×10^{-7} | 1.90×10^{-5} | 2.27×10^{-8} | 2.67×10^{-8} | 1.63×10^{-5} |
| 0.5 | 0.551456645417 | 1.07×10^{-4} | 8.58×10^{-7} | 8.58×10^{-7} | 4.33×10^{-10} | 4.33×10^{-10} | 1.64×10^{-5} |
| 0.6 | 0.582235565211 | 1.50×10^{-4} | 7.84×10^{-7} | 2.96×10^{-5} | 1.19×10^{-8} | 1.25×10^{-8} | 1.65×10^{-5} |
| 0.7 | 0.613045467313 | 2.60×10^{-4} | 9.03×10^{-7} | 1.43×10^{-5} | 1.55×10^{-8} | 3.32×10^{-9} | 1.56×10^{-5} |
| 0.8 | 0.643724157471 | 3.58×10^{-4} | 9.01×10^{-7} | 1.40×10^{-5} | 5.84×10^{-8} | 4.74×10^{-8} | 1.45×10^{-5} |
| 0.9 | 0.674050112431 | 3.04×10^{-4} | 3.94×10^{-7} | 2.86×10^{-5} | 3.83×10^{-8} | 2.66×10^{-9} | 1.50×10^{-5} |
| 1.0 | 0.703743178236 | 9.90×10^{-5} | 2.00×10^{-6} | 9.60×10^{-7} | 4.17×10^{-8} | 1.87×10^{-9} | 1.60×10^{-5} |

Table 8 Absolute error (AE) comparison of the solution of $Y_2(\zeta)$ with different values of M and k for Example 2

| ζ | NDSolve solution | The absolute error of FWCM with NDSolve | | | | | AE of FCCT with NDSolve |
|---------|------------------|---|-----------------------|-----------------------|-----------------------|------------------------|-------------------------|
| | | M=3, k=1 | M=3, k=2 | M=6, k=1 | M=6, k=2 | M=10, k=1 | |
| 0 | 1.500000000000 | 0 | 0 | 0 | 0 | 0 | 0 |
| 0.1 | 1.478490230899 | 4.02×10^{-4} | 1.82×10^{-5} | 1.39×10^{-6} | 1.23×10^{-8} | 1.58×10^{-8} | 1.12×10^{-5} |
| 0.2 | 1.453889615895 | 4.81×10^{-4} | 1.05×10^{-5} | 1.09×10^{-6} | 1.46×10^{-8} | 1.86×10^{-8} | 1.53×10^{-5} |
| 0.3 | 1.426111562473 | 4.01×10^{-4} | 1.12×10^{-5} | 1.14×10^{-6} | 2.34×10^{-8} | 2.76×10^{-8} | 1.66×10^{-5} |
| 0.4 | 1.395101995890 | 2.94×10^{-4} | 2.22×10^{-5} | 1.32×10^{-6} | 3.66×10^{-8} | 4.15×10^{-8} | 1.81×10^{-5} |
| 0.5 | 1.360847465770 | 2.52×10^{-4} | 1.38×10^{-6} | 1.38×10^{-6} | 8.86×10^{-9} | 8.86×10^{-9} | 2.03×10^{-5} |
| 0.6 | 1.323384721142 | 3.14×10^{-4} | 4.32×10^{-5} | 1.38×10^{-6} | 1.01×10^{-8} | 2.58×10^{-8} | 2.26×10^{-5} |
| 0.7 | 1.282810436334 | 4.62×10^{-4} | 2.45×10^{-5} | 1.59×10^{-6} | 1.00×10^{-8} | 8.05×10^{-9} | 2.41×10^{-5} |
| 0.8 | 1.239291331368 | 6.07×10^{-4} | 2.55×10^{-5} | 1.69×10^{-6} | 6.48×10^{-8} | 4.71×10^{-8} | 2.53×10^{-5} |
| 0.9 | 1.193072664755 | 5.81×10^{-4} | 4.78×10^{-5} | 1.20×10^{-6} | 2.92×10^{-8} | 9.46×10^{-8} | 2.79×10^{-5} |
| 1.0 | 1.144483348319 | 1.34×10^{-4} | 9.58×10^{-6} | 2.99×10^{-6} | 3.49×10^{-8} | 4.74×10^{-10} | 3.11×10^{-5} |

Table 9 Comparison of proposed approximate solution for $Y_1(\zeta)$ for different values α and β for the fractional Brussalator model (Example 2)

| ζ | $\alpha = \beta = 0.25$ | $\alpha = \beta = 0.50$ | $\alpha = \beta = 0.75$ | $\alpha = \beta = 0.98$ |
|---------|-------------------------|-------------------------|-------------------------|-------------------------|
| | FWCM (M=3, k=1) | FWCM (M=3, k=1) | FWCM (M=3, k=1) | FWCM (M=3, k=1) |
| 0 | 0.400000000000 | 0.400000000000 | 0.400000000000 | 0.400000000000 |
| 0.1 | 0.523958422225 | 0.476490264321 | 0.446848245599 | 0.430741491153 |
| 0.2 | 0.600842953464 | 0.534717827789 | 0.488823662359 | 0.461600687639 |
| 0.3 | 0.640918380821 | 0.577741508502 | 0.526468245985 | 0.492516338684 |
| 0.4 | 0.654449491299 | 0.608620124557 | 0.560323991845 | 0.523427193514 |
| 0.5 | 0.651701071926 | 0.630412494049 | 0.590932895812 | 0.554272001355 |
| 0.6 | 0.642937909735 | 0.646177435075 | 0.618836953423 | 0.584989511432 |
| 0.7 | 0.638424791741 | 0.658973765731 | 0.644578160298 | 0.615518472973 |
| 0.8 | 0.648426504987 | 0.671860304113 | 0.668698512057 | 0.645797635203 |
| 0.9 | 0.683207836495 | 0.687895868317 | 0.691740004322 | 0.675765747348 |
| 1.0 | 0.753033573295 | 0.710139276445 | 0.714244632712 | 0.705361558634 |

precision. Figures 7 and 8 depict all the graphical representations of numerical simulations and absolute error analysis. From the tables and graphs, it is clear that the FWCM method dominates all the other techniques in obtaining the numerical approximation and yields a satisfactory result for the desired model.

Example 2 We use $\lambda=0.5$ and $\delta = 0.1$ in the second model problem. In this case, we consider the nonlinear coupled system

Table 10 Comparison of proposed approximate solution for $Y_2(\zeta)$ for different values α and β for the fractional Brussalator model (Example 2)

| ζ | $\alpha = \beta = 0.25$ FWCM ($M=3, k=1$) | $\alpha = \beta = 0.50$ FWCM ($M=3, k=1$) | $\alpha = \beta = 0.75$ FWCM ($M=3, k=1$) | $\alpha = \beta = 0.98$ FWCM ($M=3, k=1$) |
|---------|---|---|---|---|
| 0 | 0.4000000000 | 0.4000000000 | 0.4000000000 | 0.4000000000 |
| 0.1 | 1.34714664734 | 1.42536212832 | 1.46213296313 | 1.47796656123 |
| 0.2 | 1.24312410548 | 1.35998486141 | 1.42257117051 | 1.45253584175 |
| 0.3 | 1.17815639304 | 1.30280268044 | 1.38157758613 | 1.42380702285 |
| 0.4 | 1.14246752863 | 1.25275006661 | 1.33941517452 | 1.39187928493 |
| 0.5 | 1.12628153089 | 1.20876150108 | 1.29634689814 | 1.35685180865 |
| 0.6 | 1.11982241844 | 1.16977146505 | 1.25263572243 | 1.31882377448 |
| 0.7 | 1.11331420995 | 1.13471443969 | 1.20854461185 | 1.27789436326 |
| 0.8 | 1.09698092396 | 1.10252490618 | 1.16433652779 | 1.23416275535 |
| 0.9 | 1.06104657906 | 1.07213734571 | 1.12027443681 | 1.18772813158 |
| 1.0 | 0.99573519400 | 1.04248623945 | 1.07662130205 | 1.13868967248 |

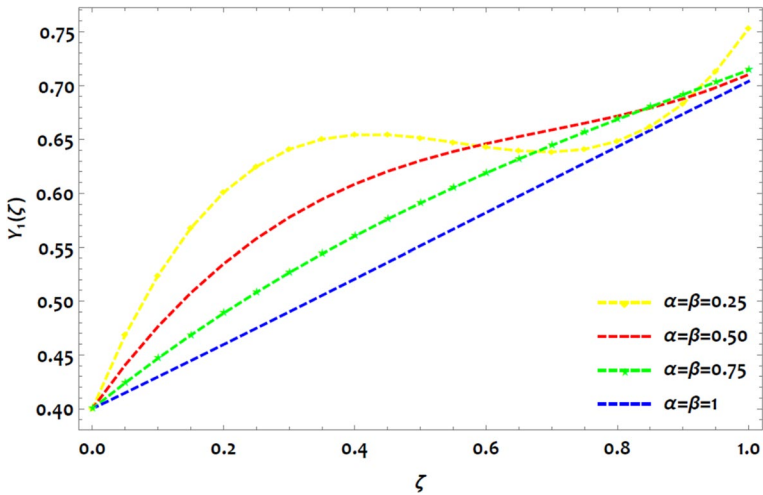


Fig. 11 Approximation of $Y_1(\zeta)$ at different values of α and β for Example 2

$$\left. \begin{aligned} D^\alpha Y_1(\zeta) &= 0.5 - 1.1Y_1(\zeta) + Y_2^2(\zeta)Y_1(\zeta) \\ D^\beta Y_2(\zeta) &= 0.1Y_1(\zeta) - Y_2^2(\zeta)Y_1(\zeta) \end{aligned} \right\} \alpha, \beta \in [0, 1] \quad (12)$$

The given initial conditions are $Y_1(0) = 0.4, Y_2(0) = 1.5$.

For $\alpha = \beta = 1, M = 3$ and $k = 1$, the following approximate solutions are obtained

$$Y_1(\zeta) = 0.4 + 0.29469634927034\zeta + 0.022860706132614\zeta^2 - 0.0137148465735597\zeta^3$$

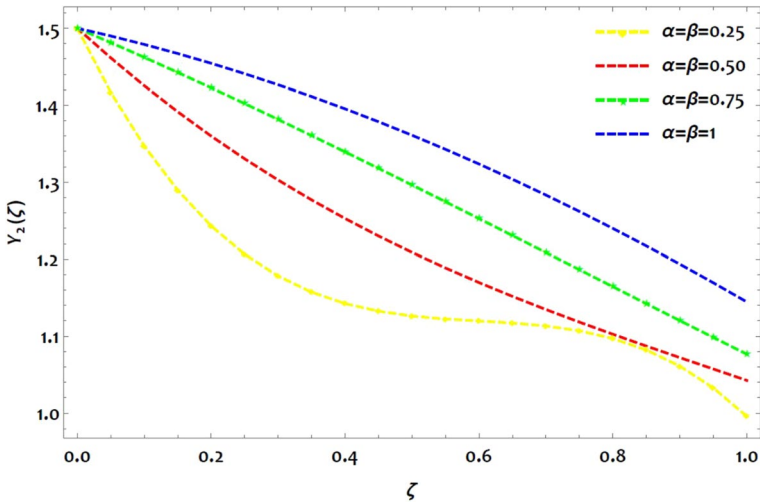


Fig. 12 Approximation of $Y_2(\zeta)$ at different values of α and β for Example 2

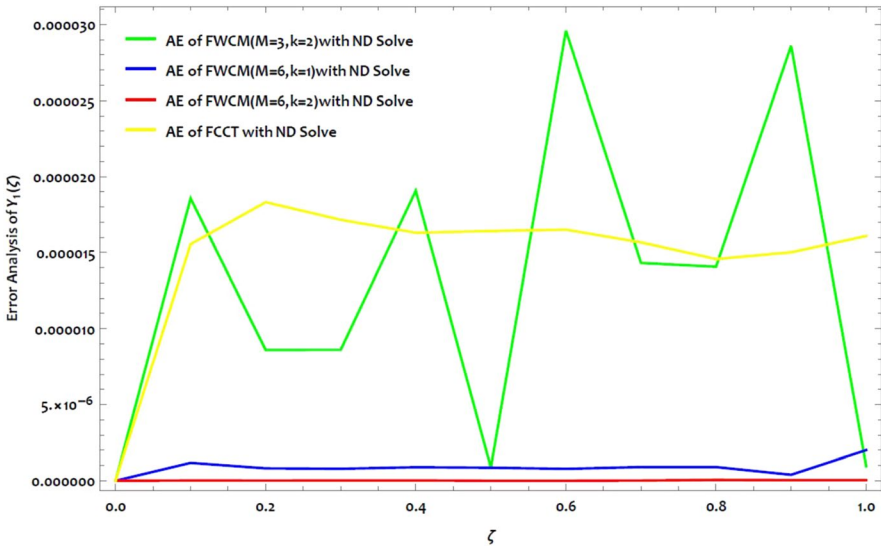


Fig. 13 Visual representation of the Absolute error comparison with different techniques for $Y_1(\zeta)$ of Example 2

$$Y_2(\zeta) = 1.5 - 0.193743929369399\zeta - 0.17459001231211\zeta^2 + 0.0129520344828012\zeta^3$$

For $\alpha = \beta = 1, M = 6$ and $k = 1$, the following approximate solutions are obtained

$$Y_1(\zeta) = 0.4 + 0.299961244480846\zeta - 0.000570073728252\zeta^2 + 0.018955737956525\zeta^3 - 0.00892306766543492\zeta^4 - 0.0067392676293283\zeta^5 + 0.00105659857034810\zeta^6$$

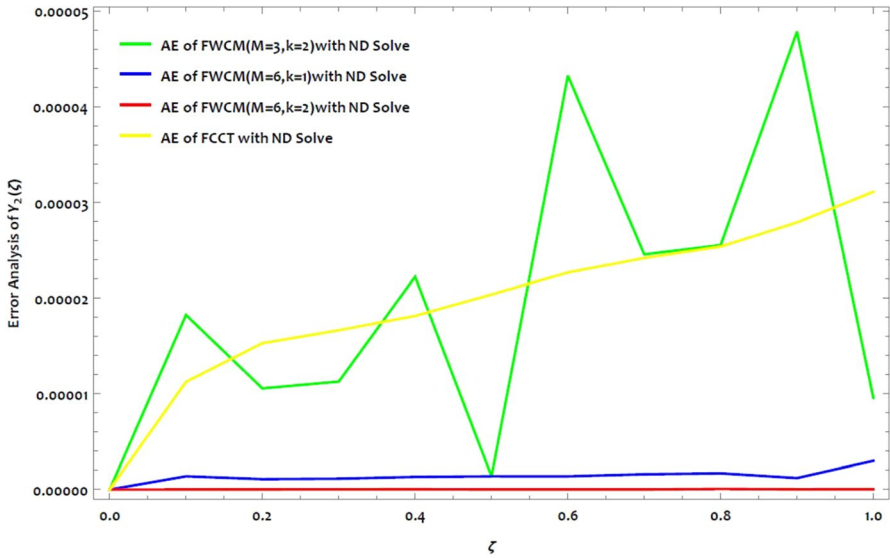


Fig. 14 Visual representation of the Absolute error comparison with different techniques for $Y_2(\zeta)$ of Example 2

$$Y_2(\zeta) = 1.5 - 0.19995756618178\zeta - 0.149452000235597\zeta^2 - 0.018559533306414\zeta^3 + 0.00365216514611315\zeta^4 + 0.0092649676596509\zeta^5 - 0.00046168658395873\zeta^6$$

For $\alpha = \beta = 0.25, M = 3$ and $k = 1$, the following approximate solutions are obtained

$$Y_1(\zeta) = 0.4 + 1.5091696334421614\zeta - 2.866933898215179\zeta^2 + 1.7107978380678157\zeta^3$$

$$Y_2(\zeta) = 1.5 - 1.8052741851107714\zeta + 2.930339608472363\zeta^2 - 1.6293302293557557\zeta^3$$

For $\alpha = \beta = 0.50, M = 3$ and $k = 1$, the following approximate solutions are obtained

$$Y_1(\zeta) = 0.4 + 0.8664122077776012\zeta - 1.0660759473792236\zeta^2 + 0.5098030160415803\zeta^3$$

$$Y_2(\zeta) = 1.5 - 0.7962334700567237\zeta + 0.5163061793996901\zeta^2 - 0.17758646989728333\zeta^3$$

For $\alpha = \beta = 0.75, M = 3$ and $k = 1$, the following approximate solutions are obtained

$$Y_1(\zeta) = 0.4 + 0.49465325224797463\zeta - 0.27074122296067227\zeta^2 + 0.09033260342514833\zeta^3$$

$$Y_2(\zeta) = 1.5 - 0.36932004327547263\zeta - 0.0978859874431673\zeta^2 + 0.04382733276706626\zeta^3$$

The FWCM solutions for Example 2 were obtained for the values of $\alpha = \beta = 1$ are shown in Figs. 9 and 10, revealing that the proposed method solutions are reasonably close to the NDSolve results compared to the existing method Fractional clique collocation (FCC) technique. The FWCM obtained numerical approximations compared with the NDSolve solution (due to the unavailability of the exact solution). Absolute errors of the developed approach with the NDSolve solution are tabulated in Tables 7 and 8. It is easy to see that the errors obtained using the proposed FWCM method are lesser than those obtained using other existing techniques. The numerical approximation of the model at different values of α and β are computed and listed in Tables 9 and 10. The graphical representation of the solution at $\alpha = \beta = 0.25$, $\alpha = \beta = 0.50$, $\alpha = \beta = 0.75$, and $\alpha = \beta = 1$, respectively drawn on the Figs. 11 and 12. FWCM solutions are calculated at different values of M and k . Also, by increasing the values of M and k , we get further precision in the result, which can be seen in Tables 7 and 8. It indicates we can get a higher-order accuracy by increasing M and k . Figures 13 and 14 depict all the graphical representations of numerical simulations and absolute error analysis. From the tables and graphs, it is clear that the FWCM method dominates all the other techniques in obtaining the numerical approximation and yields a satisfactory result for the desired model.

6 Conclusion

This study uses the Fibonacci wavelet collocation method to derive an effective and accurate approximate solution for the nonlinear Brusselator system of equations of fractional order arising in chemical engineering. Based on the Fibonacci wavelets, a new operational matrix is created for different resolutions (k) and combined with the collocation technique to solve the model numerically. The work presented here shows how the FWCM can be used to solve systems of differential equations of fractional order. The outcomes of this approach are well-aligned with the ND solver in Mathematica. The findings in the tables and figures show that the suggested method is more accurate than the currently used numerical models. Also, numerical illustrations support the claim that only a few Fibonacci wavelets are sufficient to attain suitable outcomes. The method yielded a very excellent result while being simple to use. It underlined our conviction that the method is a convenient method for handling fractional differential equations that are highly nonlinear. The technique that is being discussed is simple, uncomplicated to use, and requires less computation.

Acknowledgements Dr. Kumbinarasaiah S expresses his affectionate thanks to the DST-SERB, Govt. of India, New Delhi for the financial support under Empowerment and Equity Opportunities for Excellence in Science for 2023–2026. F. No. EEQ/2022/620 Dated: 07/02/2023.

Author contributions KS proposed the main idea of this paper. KS and MG prepared the manuscript and performed all the steps of the proofs in this research. Both authors contributed equally and significantly to writing this paper. Both authors read and approved the final manuscript.

Funding The author states that no funding is involved.

Data availability The data supporting this study's findings are available within the article.

Declarations

Competing interests The authors declare that they have no competing interests.

References

1. I. Prigogine, R. Lefever, Symmetry breaking instabilities in dissipative systems. II. *J. Chem. Phys.* **48**(4), 1695–1700 (1968)
2. S. Momani, Z. Odibat, Analytical approach to linear fractional partial differential equations arising in fluid mechanics. *Phys. Lett. A* **355**(4–5), 271–279 (2006)
3. H. Xu, A generalized analytical approach for highly accurate solutions of fractional differential equations. *Chaos Solitons Fract.* **166**, 112917 (2023)
4. Z. Odibat, S. Kumar, A robust computational algorithm of homotopy asymptotic method for solving systems of fractional differential equations. *J. Comput. Nonlinear Dyn.* **14**(8), 081004 (2019)
5. H.A. Alkresheh, A.I. Ismail, Multi-step fractional differential transform method for the solution of fractional order stiff systems. *Ain Shams Eng. J.* **12**(4), 4223–4231 (2021)
6. O. Abdulaziz, I. Hashim, S. Momani, Solving systems of fractional differential equations by homotopy-perturbation method. *Phys. Lett. A* **372**(4), 451–459 (2008)
7. M.Y. Ongun, D. Arslan, R. Garrappa, Nonstandard finite difference schemes for a fractional-order Brusselator system. *Adv. Differ. Equ.* **2013**, 1–13 (2013)
8. Z.U.A. Zafar, K. Rehan, M. Mushtaq, M. Rafiq, Numerical treatment for nonlinear Brusselator chemical model. *J. Differ. Equ. Appl.* **23**(3), 521–538 (2017)
9. H. Jafari, A. Kadem, D. Baleanu, Variational iteration method for a fractional-order Brusselator system. In *Abstract and Applied Analysis*, vol. 2014. Hindawi.
10. C. Bota, B. Căruntu, Approximate analytical solutions of the fractional-order brusselator system using the polynomial least squares method. *Adv. Math. Phys.* (2015)
11. H. Khan, H. Jafari, R.A. Khan, H. Tajadodi, S.J. Johnston, Numerical solutions of the nonlinear fractional-order Brusselator system by Bernstein polynomials. *Sci. World J.* (2014)
12. P. Chang, A. Isah, Legendre wavelet operational matrix of fractional derivative through wavelet-polynomial transformation and its applications in solving fractional Order Brusselator system. *J. Phys.* **693**(1), 012001 (2016)
13. M. Izadi, H.M. Srivastava, Fractional clique collocation technique for numerical simulations of fractional-order Brusselator chemical model. *Axioms* **11**(11), 654 (2022)
14. V. Gafiychuk, B. Datsko, Stability analysis and limit cycle in fractional system with Brusselator nonlinearities. *Phys. Lett. A* **372**(29), 4902–4904 (2008)
15. L.G. Yuan, J.H. Kuang, Stability and a numerical solution of fractional-order Brusselator chemical reaction system. *J. Fract. Calc. Appl* **8**(1), 38–47 (2017)
16. R.K. Asv, S. Devi, A novel three-step iterative approach for oscillatory chemical reactions of fractional brusselator model. *Int. J. Modell. Simul.* 1–20. (2022)
17. A.A. Alderremy, R. Shah, N. Iqbal, S. Aly, K. Nonlaopon, Fractional series solution construction for nonlinear fractional reaction-diffusion Brusselator model utilizing laplace residual power series. *Symmetry* **14**(9), 1944 (2022)
18. W. Beghami, B. Maayah, O.A. Arqub, S. Bushnaq, Fractional approximate solutions of 2D reaction–diffusion Brusselator model using the novel Laplace-optimized decomposition approach. *Int. J. Mod. Phys. C* **34**, 2350086 (2022)
19. A. Anber, Z. Dahmani, Solutions of the reaction-diffusion Brusselator with fractional derivatives. *J. Interdiscip. Math.* **17**(5–6), 451–460 (2014)
20. S. Dhawan, J.A.T. Machado, D.W. Brzeziński, M.S. Osman, A Chebyshev wavelet collocation method for some types of differential problems. *Symmetry* **13**(4), 536 (2021)
21. M. Faheem, A. Raza, A. Khan, Collocation methods based on Gegenbauer and Bernoulli wavelets for solving neutral delay differential equations. *Math. Comput. Simul.* **180**, 72–92 (2021)

22. S. Kumbinarasaiah, K.R. Raghunatha, The applications of Hermite wavelet method to nonlinear differential equations arising in heat transfer. *Int. J. Thermofluids* **9**, 100066 (2021)
23. S. Kumbinarasaiah, R.A. Mundewadi, Numerical solution of fractional-order integro-differential equations using Laguerre wavelet method. *J. Inf. Optim. Sci.* **43**(4), 643–662 (2022)
24. S. Erman, A. Demir, E. Ozbilge, Solving inverse nonlinear fractional differential equations by generalized Chelyshkov wavelets. *Alex. Eng. J.* **66**, 947–956 (2023)
25. X. Li, Numerical solution of fractional differential equations using cubic B-spline wavelet collocation method. *Commun. Nonlinear Sci. Numer. Simul.* **17**(10), 3934–3946 (2012)
26. A. Isah, C. Phang, Genocchi wavelet-like operational matrix and its application for solving nonlinear fractional differential equations. *Open Phys.* **14**(1), 463–472 (2016)
27. T.N. Vo, M. Razzaghi, P.T. Toan, Fractional-order generalized Taylor wavelet method for systems of nonlinear fractional differential equations with application to human respiratory syncytial virus infection. *Soft. Comput.* **26**, 165–173 (2022)
28. T. Abdeljawad, R. Amin, K. Shah, Q. Al-Mdallal, F. Jarad, Efficient sustainable algorithm for numerical solutions of systems of fractional order differential equations by Haar wavelet collocation method. *Alex. Eng. J.* **59**(4), 2391–2400 (2020)
29. J. Xie, T. Wang, Z. Ren, J. Zhang, L. Quan, Haar wavelet method for approximating the solution of a coupled system of fractional-order integral–differential equations. *Math. Comput. Simul.* **163**, 80–89 (2019)
30. E. Keshavarz, Y. Ordokhani, M. Razzaghi, Bernoulli wavelet operational matrix of fractional order integration and its applications in solving the fractional order differential equations. *Appl. Math. Model.* **38**(24), 6038–6051 (2014)
31. S. Kumbinarasaiah, G. Manohara, G. Hariharan, Bernoulli wavelets functional matrix technique for a system of nonlinear singular Lane Emden equations. *Math. Comput. Simul.* **204**, 133–165 (2022)
32. H.M. Srivastava, F.A. Shah, N.A. Nayied, Fibonacci wavelet method for the solution of the nonlinear Hunter-Saxton equation. *Appl. Sci.* **12**(15), 7738 (2022)
33. S. Kumbinarasaiah, Hermite wavelets approach for the multi-term fractional differential equations. *J. Interdiscip. Math.* **24**(5), 1241–1262 (2021)
34. Y. Chen, X. Ke, Y. Wei, Numerical algorithm to solve a system of nonlinear fractional differential equations based on wavelets method and the error analysis. *Appl. Math. Comput.* **251**, 475–488 (2015)
35. A. Secer, S. Altun, A new operational matrix of fractional derivatives to solve systems of fractional differential equations via Legendre wavelets. *Mathematics* **6**(11), 238 (2018)
36. F. Mohammadi, C. Cattani, A generalized fractional-order Legendre wavelet Tau method for solving fractional differential equations. *J. Comput. Appl. Math.* **339**, 306–316 (2018)
37. L.I. Yuanlu, Solving a nonlinear fractional differential equation using Chebyshev wavelets. *Commun. Nonlinear Sci. Numer. Simul.* **15**(9), 2284–2292 (2010)
38. M. ur Rehman, U. Saeed, Gegenbauer wavelets operational matrix method for fractional differential equations. *J. Korean Math. Soc.* **52**(5), 1069–1096 (2015)
39. D.Q. Dai, W. Lin, Orthonormal polynomial wavelets on the interval. *Proc. Am. Math. Soc.* **134**(5), 1383–1390 (2006)
40. T. Kilgore, J. Prestin, Polynomial wavelets on the interval. *Constr. Approx.* **12**, 95–110 (1996)
41. F.A. Shah, M. Irfan, K.S. Nisar, R.T. Matoog, E.E. Mahmoud, Fibonacci wavelet method for solving time-fractional telegraph equations with Dirichlet boundary conditions. *Results Phys.* **24**, 104123 (2021)
42. S. Kumbinarasaiah, M. Mulimani, A novel scheme for the hyperbolic partial differential equation through Fibonacci wavelets. *J. Taibah Univ. Sci.* **16**(1), 1112–1132 (2022)
43. S. Sabermahani, Y. Ordokhani, S.A. Yousefi, Fibonacci wavelets and their applications for solving two classes of time-varying delay problems. *Optim. Control Appl. Methods* **41**(2), 395–416 (2020)
44. S. Kumbinarasaiah, M. Mulimani, Fibonacci wavelets approach for the fractional Rosenau-Hyman equations. *Results Control Optim.* **11**, 100221 (2023)
45. M. Kumar, K.N. Rai, Numerical simulation of time-fractional bioheat transfer model during cryosurgical treatment of skin cancer. *Comput. Therm. Sci.* **13**(4) (2021)
46. S. Kumbinarasaiah, M. Mulimani, Fibonacci wavelets-based numerical method for solving fractional order (1+1)-dimensional dispersive partial differential equation. *Int. J. Dyn. Control* 1–24 (2023)

47. W.M. Abd-Elhameed, Y.H. Youssri, A novel operational matrix of Caputo fractional derivatives of Fibonacci polynomials: spectral solutions of fractional differential equations. *Entropy* **18**(10), 345 (2016)
48. S.C. Shiralashetti, L. Lamani, Fibonacci wavelet-based numerical method for solving nonlinear Stratonovich Volterra integral equations. *Sci. Afr.* **10**, e00594 (2020)
49. S. Abdi-Mazraeh, H. Kheiri, S. Irandoust-Pakchin, Construction of operational matrices based on linear cardinal B-spline functions for solving fractional stochastic integro-differential equation. *J. Appl. Math. Comput.* 1–25 (2021)
50. S. Irandoust-pakchin, M. Dehghan, S. Abdi-mazraeh, M. Lakestani, Numerical solution for a class of fractional convection–diffusion equations using the flatlet oblique multiwavelets. *J. Vib. Control* **20**(6), 913–924 (2014)
51. M.V. Salehian, S. Abdi-mazraeh, S. Irandoust-pakchin, N. Rafati, Numerical solution of Fokker-Planck equation using the flatlet oblique multiwavelets. *Int. J. Nonlinear Sci.* **13**(4), 387–395 (2012)
52. M. Lakestani, M. Dehghan, S. Irandoust-Pakchin, The construction of operational matrix of fractional derivatives using B-spline functions. *Commun. Nonlinear Sci. Numer. Simul.* **17**(3), 1149–1162 (2012)
53. M. Kumar, S. Pandit, Wavelet transform and wavelet based numerical methods: an introduction. *Int. J. Nonlinear Sci.* **13**(3), 325–345 (2012)
54. S. Kumbinaraiaiah, G. Manohara, Modified Bernoulli wavelets functional matrix approach for the HIV infection of CD4+ T cells model. *Results Control Optim.* **10**, 100197 (2023)

Publisher's Note Springer Nature remains neutral with regard to jurisdictional claims in published maps and institutional affiliations.

Springer Nature or its licensor (e.g. a society or other partner) holds exclusive rights to this article under a publishing agreement with the author(s) or other rightsholder(s); author self-archiving of the accepted manuscript version of this article is solely governed by the terms of such publishing agreement and applicable law.